EXHIBIT A

IN THE UNITED STATES PATENT AND TRADEMARK OFFICE

In re application of:	Confirmation No.: 6653
SCHENK, Dale B.	Examiner: K. Ballard, Ph.D.
Application No.: 09/724,319	Art Unit: 1649
Filed: November 27, 2000	DECLARATION OF DR. PETER SEUBERT UNDER 37 C.F.R. §1.131
For: PREVENTION AND TREATMENT OF AMYLOIDOGENIC DISEASE	

Commissioner for Patents
P.O. Box 1450
Alexandria, VA 22313-1450

Sir:

I, Peter Seubert, state as follows:

1. My current position is Vice President, Neurodegenerative Research at Elan Pharmaceuticals, Inc., the assignee of the above-captioned application. A copy of my curriculum vitae is attached.

2. I understand that Solomon, US Patent No. 5,688,651 reports that an antibody designated AMY-33 has a putative epitope between residues 25-28 of Aβ. I understand this putative assignment is based on AMY-33 being raised against a 1-28 fragment of Aβ, and Yankner et al., Science 250:279-282 (1990) having speculated that residues 25-35 of Aβ mediated toxic effects. The putative epitope 25-28 represents the intersection of the fragment generating AMY-33 with the 25-35 toxic region hypothesized by Yankner et al.

3. I or others acting under my supervision have performed the following experiment to determine the epitope specificity of the AMY-33 antibody. We obtained the antibody from Zymed Laboratories, Inc (now Invitrogen).

4. The following peptides were used for analysis. Aβ1-10 C-terminally biotinylated obtained from Mimotopes; Aβ1-16 N-terminally biotinylated obtained from Anaspec; Aβ 13-28 biotinylated through a C-terminal cysteine using Pierce's no weigh maleimide PEO2-Biotin at a 10 M ratio; and, Aβ 1-38 biotinylated using Pierce's NHS PEO2 Biotin at a 5 M ratio following ForteBio's recommended biotinylation protocol. Binding was detected using a Fortebio's Octet, which is a label-free instrument for determining both binding and kinetics of protein-protein interactions. For this experiment, the Fortebio Strepavidin High binding FA Biosensors were loaded with 5 μg/ml of the different biotinylated Aβ peptides. The sensors were then allowed to reach baseline before the association and dissociation and K_D of each antibody was determined. Antibodies were run at molar concentrations of 1-10 times their expected K_D. Various antibodies whose epitope specificity had previously been determined, specifically 2H3 (epitope =Aβ2-7) and 12A11 (epitope =Aβ3-7), were used as a positives control for various n terminal peptides and Aβ 1-38: antibody 266 (epitope =Aβ16-23) was used as the positive control for 13-28 and 6H9(epitope Aβ19-22) was used as the positive control for Aβ17-28.

5. The table below shows the measured affinity of AMY33 for the various fragments of Aβ tested. In brief, AMY33 showed binding to Aβ 1-10, 1-16 and 1-38 at approximately 100 fold less affinity than the control antibody 12A11 but showed no detectable binding to Aβ13-28 and 17-28.

		BINDING AFFINITY				
		K_D Aβ 1-10	K_D Aβ 1-16	K_D Aβ 1-38	K_D Aβ 13-28	K_D Aβ 17-28
ANTIBODY	AMY 33	100-300 nM	100-300 nM	100-300 nM	No binding	No binding
	12A11	Not done	1-2 nM	1-3 nM	No binding	No binding
	2H3	0.6 nM	0.2 nM	0.45 nM	Not done	Not done
	266	Not done	Not done	Not done	0.15 nM	Not done
	6H9	Not done	Not done	Not done	0.6 nM	Not done

6. I conclude from the detectable binding to Aβ1-10 and lack of detectable binding to the Aβ13-28 fragment that the epitope bound by AMY-33 does not lie within residues 13-28 of Aβ.

7. I further declare that all statements made herein of my own knowledge are true and that all statements made on information and belief are believed to be true; and further that these statements were made with the knowledge that willful false statements and the like so made are punishable by fine or imprisonment, or both, under Section 1001 of Title 18 of the United States Code, and that such willful false statements may jeopardize the validity of the application or any patent issuing thereon.

Respectfully submitted,

Peter Seubert

Date: October 11, 2007

TOWNSEND and TOWNSEND and CREW LLP
Two Embarcadero Center, Eighth Floor
San Francisco, California 94111-3834
Tel: (650) 324-2600
Fax: (415) 576-0300
JOL:RLC:sjj
61173279 v1

CURRICULUM VITAE

Peter Seubert, Ph.D

Home Address
801 Castro St..
San Francisco, CA 94114

Business Address
Elan Pharmaceuticals, Inc.
800 Gateway Boulevard
South San Francisco, California 94080

EDUCATION

1984 **Ph.D., Biochemistry**, University of California, Davis
Dissertation Title: Functional studies of ATP sulfurylase from *Penicillium chrysogenum*
Advisor: Dr. Irwin H. Segel

1979 **B.S., Biochemistry**, University of California, Davis

SCIENTIFIC BACKGROUND

1989-present **Vice President Biology Research**, Elan Pharmaceuticals, South San Francisco, California.
Discovery and development of biochemical tests for the diagnosis of Alzheimer's disease. Studies of the metabolism and aberrant deposition of the amyloid protein and microtubule associated protein tau. Characterization of inhibitors of amyloid formation in neuronal culture and transgenic mouse model of Alzheimer's disease. Development of vaccine-based approach to Alzheimer's disease treatment.

1988-1989 **Scientific Consultant**, Cortex Pharmaceuticals, Inc., Irvine, California.

1985-1989 **Postdoctoral Fellow and Assistant Researcher**, Bonney Center for the Neurobiology of Learning and Memory, University of California, Irvine; laboratory of Dr. Gary Lynch. Investigation of the role of calcium-activated proteases in memorial and pathological neuronal events. Demonstration of intracellular proteolysis of brain spectrin coupled to activation of NMDA receptors during ischemia and in response to toxins, lesions, and in certain hereditary disorders. Biochemical studies of roles of calcium activated

proteins (calpain, protein kinase C, calmodulin) in neuronal plasticity and degeneration.

1979-1984 **Graduate Student**, Department of Biochemistry and Biophysics, University of California, Davis. Studies of sulfate activating enzymes: ATP sulfurylase and adenosine 5'-phosphosulfate kinase. Initial velocity, product inhibition, inhibition by substrate analogs, analysis of reaction progress curves by a simplified integrated rate equation, alternative substrates, and equilibrium binding studies used to deduce kinetic mechanisms and ligand binding order of the sulfate activating enzymes.

1978-1979 **Undergraduate Student**, Department of Biochemistry and Biophysics, University of California, Davis; under direction of Dr. Irwin H. Segel. Isolation and preliminary characterization of ATP sulfurylase from mammalian source and thermophilic fungus for comparative studies with mesophilic fungus enzyme.

AWARDS AND HONORS

- National Institute on Aging Postdoctoral Training Fellowship 1985
- Jastro-Shields Research Scholarship Awards 1978, 1979, 1982, 1983
- University of California Regents' Fellowship 1982
- Earl C. Anthony Fellowship 1981
- Outstanding Teaching Assistant in Biochemistry Award 1981
- Henry A. Jastro Scholar in Biochemistry Award 1980
- Andrew Christensen Scholarship 1979
- Outstanding Undergraduate Achievement in Biochemistry Citation 1979
- Graduation with high honors, University of California, Davis 1979

[ps\cv]

PUBLICATIONS

1. Farley, J.R., Christie, E.A., Seubert, P.A., and Segel, I.H. (1979) Adenosinetriphosphate sulfurylase from *Penicillium chrysogenum*: Evidence for essential arginine, histidine and tyrosine residues. J. Biol. Chem., 254:3537-3542.

2. Seubert, P.A., Grant, P.A., Christie, E.A., Farley, J.R., and Segel, I.H. (1980) Kinetic and chemical properties of ATP sulphurylase from *Penicillium chrysogenum*. In: Sulphur in Biology, Ciba Foundation Symposium, 72:19-47.

3. Seubert, P.A., Hoang, L., Renosto, F., and Segel, I.H. (1983) ATP sulfurylase from *Penicillium chrysogenum*: measurements of the true specific activity of an enzyme subject to potent product inhibition and reassessment of the kinetic mechanism. Arch. Biochem. Biophys., 225:679-691.

4. Renosto, F., Seubert, P.A., and Segel, I.H. (1984) Adenosine 5'-phosphosulfate kinase form *Penicillium chrysogenum*: purification and kinetic characterization. J. Biol. Chem., 259:2113-2123.

5. Renosto, F., Seubert, P.A., Knudson, P., and Segel, I.H. (1985) APS kinase form *Penicillium chrysogenum*: dissociation and reassociation of subunits as the basis of the reversible heat inactivation. J. Biol. Chem., 260:1535-1544.

6. Seubert, P.A., Renosto, F., Knudson, P., and Segel, I.H. (1985) Adenosinetriphosphate sulfurylase from *Penicillium chrysogenum*: steady-state kinetics of the forward and reverse reractions, alternate substrate kinetics, and equilibrium binding studies. Arch. Biochem. Biophys., 240:509-523.

7. Segel, I.H., Renosto, R., and Seubert, P.A. (1987) The sulfate activating enzymes. Methods in Enzymology, 143:333-349.

8. Seubert, P., Baudry, M., Dudek, S. and Lynch, G. (1987) Calmodulin stimulates the degradation of brain spectrin by calpain. Synapse, 1:20-24.

9. Baudry, M., Seubert, P. and Lynch, G. (1987) A possible second messenger system for the production of long-term changes in synapses. In: Molecular Mechanisms of Neuronal Responsiveness (Y.H. Ehrlich, R.H. Lenox, E. Kornecki, W.O. Berry, ed.). Plenum Press, New York and London, 291-311.

10. Perlmutter, L., Siman, R., Gall, C., Seubert, P., Baudry, M. and Lynch, G. (1988) Ultrastructural localization of calcium-activated proteases (calpain) in rat brain. Synapse, 2:79-88.

11. Ivy, G.O., Seubert, P., Baudry, M. and Lynch, G. (1988) Presence of brain spectrin in dendrites of mammalian brain: technical factors involved in immunocytochemical detection. Synapse, 2:329-333.

12. Seubert, P., Ivy, G., Larson, J., Lee, J., Shahi, K., Baudry, M. and Lynch, G. (1988) Lesions of entorhinal cortex produce a calpain-mediated degradation of brain spectrin in dentate gyrus. I. Biochemical studies. Brain Res., 459:226-233.

13. Ivy, G., Seubert, P., Lynch, G. and Baudry, M. (1988) Lesions of entorhinal cortex produce a calpain-mediated degradation of brain spectrin in dentate gyrus. II. Anatomical studies. Brain Res., 459:233-241.

14. Seubert, P., Larson, J., Oliver, M., Jung. M.W., Baudry, M. and Lynch, G. (1988) Stimulation of NMDA receptors induces proteolysis of spectrin in hippocampus. Brain Res., 460:189-195.

15. Lynch, G., Muller, D., Seubert, P., and Larson, J. (1988) Long-term potentiation: persisting problems and recent results. Brain Res. Bull., 21:363-372.

16. Lynch, G., Seubert, P. (1989) Links between long-term potentiation and neuropathology: an hypothesis involving calcium-activated proteases. Annals of the New York Academy of Sciences, Vol. 568. In: Calcium, Membranes, Aging, and Alzheimer's Disease (Khachaturian, A.S. Cotman, C.W., and Pettegrew, J.W., eds.) New York Academy of Scineces, NY, 568:171-180.

17. Seubert, P., Nakagawa, Y., Ivy, G., Vanderklish, P., Lynch, G., and Baudry, M. (1989) Intrahippocampal colchicine injection results in spectrin proteolysis. Neurosci. 31:195-202.

18. Seubert, P., Lee, K., and Lynch, G. (1989) Ischemia triggers NMDA receptor-linked cytoskeletal proteolysis in hippocampus. Brain Res., 492:366-370.

19. Seubert, P., Peterson, C., Vanderklish, P., and Lynch, G. (1990) Elevated levels of brain spectrin proteolysis in the Brindled mouse. Neurosci. Lett. 108:303-308.

20. Seubert, P. and Lynch, G. (1990) Plasticity to pathology: brain calpains as modifiers of synaptic structure. In: Intracellular calcium-dependent

[ps\cv]

proteolysis (R.L. Mellgren and T. Murachi, eds.) CRC Press, Boca Raton, 251-264.

21. Sinha, S., Dovey, H.F., Seubert, P., Ward, P.J., Blacher, R.W., Blaber, M., Bradshaw, R.A., Arici, M., Mobley, W.C., and Lieberburg, I. (1990) The protease inhibitory properties of the Alzheimer' s β-amyloid precursor protein. J. Biol. Chem. 265:8983-8985.

22. Peterson, C., Vanderklish, P., Seubert, P., Cotman, C. and Lynch, G. (1991) Increased spectrin proteolysis in fibroblasts from aged and Alzheimer donors. Neurosci. Lett. 121:239-243.

23. Schenk, D., Seubert, P., Johnson-Wood, K., Lieberburg, I., (1991) Biochemical markers for Alzheimer disease. Bull. Clin. Neurosci. 56:161-167.

24. Seubert, P., Vigo-Pelfrey, C., Esch, F., Lee, M., Dovey, H., Davis, D., Sinha, S., Schlossmacher, M., Whaley, J., Swindlehurst, C., McCormack, R., Wolfert, R., Selkoe, D., Lieberburg, I., Schenk, D. (1992) Isolation and quantitation of soluble Alzheimer's beta-peptide from biological fluids. Nature 359:325-327.

25. Citron, M., Oltersdorf, T., Haass, C., McConlogue, L., Hung, A.Y., Seubert, P., Vigo-Pelfrey, C., Lieberburg, I., Selkoe, D.J. (1992) Mutation of the beta-amyloid precursor protein in familial Alzheimer's disease increases beta-protein production. Nature 360:672-674.

26. Seubert, P., Oltersdorf, T., Lee, M.G., Barbour, T., Blomquist, C., Davis, D.L., Bryant, K., Fritz, L.C., Galasko, D., Thal L.J., Lieberburg, I., Schenk, D.B. (1993) Secretion of beta-amyloid precursor protein cleaved at the amino terminus of the beta-amyloid peptide. Nature 361:260-263.

27. Johnson-Wood, K.L., Henriksson, T., Seubert, P., Oltersdorf, T., Lieberburg, I., Schenk, D.B. (1994) Identification of secreted beta-amyloid precursor binding sites on intact human fibroblasts. Biochem. Biophys. Res. Comm. 200:1685-1695.

28. Seubert, P., Schenk, D. (1994) Recent advances in identifying markers of Alzheimer's disease. In: Facts and Research in Gerontology, Volume 7. (L.J. Fitten, ed.) Serdi, Paris, 31-37.

29. Knops, J., Suomensaari, S., Lee, M., McConlogue, L., Seubert, P., Sinha, S. (1995) Cell-type and amyloid precursor protein-type specific inhibition of amyloid beta release by bafilomycin A1, a selective inhibitor of vacuolar ATPases. J. Biol. Chem. 270:2419-2422.

[ps\cv]

30. Vigo-Pelfrey, C., Seubert, P., Barbour, R., Blomquist, C., Lee, M., Lee, D., Coria, F., Chang, L., Miller, B., Lieberburg, I., Schenk, D., (1995) Elevation of microtubule-associated protein tau in the cerebrospinal fluid of patients with Alzheimer's disease. Neurology 45:788-793.

31. Seubert, P., Mawal-Dewan, M., Barbour, R., Jakes, R., Goedert, M., Johnson, G.V., Littersky, J.M., Schenk, D., Lieberburg, I., Trojanowski, J.Q., Lee, V.M.-Y. (1995) Detection of phosphorylated Ser262 in fetal tau, adult tau and paired helical filament tau. J. Biol. Chem. 270:18,917-18,922.

32. Motter, R., Vigo-Pelfrey, C., Kholodenko, D., Barbour, R., Johnson-Wood, K., Galasko, D., Chang, L., Miller, B., Clark, C., Green, R., Olson, D., Southwick, P., Wolfert, R., Munroe, B., Lieberburg, I., Seubert, P., Schenk, D. (1995) Reduction of beta-amyloid peptide42 in the cerebrospinal fluid of patients with Alzheimer's disease. Ann. Neurol. 38:643-648.

33. Games, D., Adams, D., Alessandrini, R., Barbour, R., Berthelette, P., Blackwell, D., Carr, T., Clemens, J., Donaldson, T., Gillespie, F., Guido, T., Hagopian, S., Johnson-Wood, K., Khan, K., Lee, M., Leibowitz, P., Lieberburg, I., Little, S., Masliah, E., McConlogue, L., Montoya-Zavala, M., Mucke, L., Paganini, L., Penniman, E., Power, M., Schenk, D., Seubert, P., Snyder, B., Soriano, F., Tan, H., Vitale, J., Wadsworth, S., Wolozin, B., Zhao, J. (1995) Alzheimer-type neuropathology in transgenic mice overexpressing V717F beta-amyloid precursor protein. Nature 373:523-527.

34. Haass, C., Lemere, C.A., Capell, A., Citron, M., Seubert, P., Schenk, D., Lannfelt, L., Selkoe, D.J. (1995) The Swedish mutation causes early-onset Alzheimer's disease by β-secretase cleavage within the secretory pathway. Nature Med. 1:1291-1296.

35. Seubert, P., Galasko, D., Boss, M.A. (1996) Use of CSF-based markers in the diagnosis of Alzheimer's disease. In: Pharmacological Treatment of Alzheimer's Disease: Molecular and Neurobiological Foundations (J.C. Brioni and M.W. Decker, eds.) John Wiley & Sons, Inc., New York, 345-366.

36. Litersky, J.M., Johnson, G.V.W., Jakes, R., Goedert, M., Lee, M., Seubert, P. (1996) Tau protein is phosphorylated by cAMP-dependent protein kinase and calcium/calmodulin protein kinase II within its microtubule-binding domains at Ser262 and Ser356. Biochem. J. 316:655-660.

37. Seubert, P. (1996) Commentary: Diagnosing Alzheimer's Disease: Tapping into new ideas. Alzheimer's Disease Review 1:84-86.

[ps\cv]

38. Citron, M., Diehl, T.S., Gordon, G., Biere, A.L., Seubert, P., Selkoe, D.J. (1996) Evidence that the 42- and 40-amino acid forms of amyloid ß protein are generated from the ß-amyloid precursor protein by different protease activities. Proc. Natl. Acad. Sci. USA. 93:13170-13175.

39. Schenk, D., Lieberburg, I., Motter, R., Seubert, P., (1996) The effect of Apolipoprotein E genotype on biochemical markers of Alzheimer's disease. Ann. New York Acad. Sci. 802:92-100.

40 Johnson, G.V.W., Seubert, P., Cox, T.M., Motter, R., Brown, J.P., Galasko, D. (1997) The tau protein in human cerebrospinal fluid in Alzheimer's disease consists of proteolytically derived fragments. J. Neurochem. 68:430-433.

40. Citron, M., Westaway, D., Xia, W., Carlson, G., Diehl, T., Levesque, G., Johnson-Wood, K., Lee, M., Seubert, P., Davis, A., Kholodenko, D., Motter, R., Sherrington, R., Perry, B., Yao, H., Strome, R., Lieberburg, I., Rommens, J., Kim, S., Schenk, D., Fraser, P., St George Hyslop, P., Selkoe, D.J. (1997) Mutant presenillins of Alzheimer's disease increase production of 42-residue amyloid ß-protein in both transfected cells and transgenic mice. Nature Med. 3:67-72.

41. Galasko, D., Clark, C., Chang, L., Miller, B., Green, R.C., Motter, R., Seubert, P. (1997) Assessment of cerebrospinal fluid levels of tau protein in mildly demented patients with Alzheimer's disease. Neurology 48:632-635.

42. Qiu, W.Q., Ye, Z., Kholodenko, D., Seubert, P., Selkoe, D.J. (1997) Degradation of amyloid beta-protein by a metalloprotease secreted by microglia and other neural and non-neural cells. J. Biol. Chem. 272:6641-6646.

43. Johnson-Wood, K., Lee, M., Motter, R., Hu, K., Gordon, G., Barbour, R., Khan, K., Gordon, M., Tan, H., Games, D., Lieberburg, I., Schenk, D., Seubert, P., McConlogue, L. (1997) Amyloid precursor protein processing and Aß42 deposition in a transgenic mouse model of Alzheimer's disease. Proc. Natl. Acad. Sci. USA. 94:1550-1555

44. Xia, W., Zhang, J., Kholodenko, D., Citron, M., Podlisny, M.B., Teplow, D.B., Haass, C., Seubert, P., Koo, E.H., Selkoe, D.J. (1997) Enhanced production and oligomerization of the 42-residue amyloid ß-protein by Chinese hamster ovary cells stably expressing mutant presenilins. J. Biol. Chem. 272:7977-7982.

[ps\cv]

45. Podlisny, M., Citron, M., Amarante, P., Sherrington, R., Xia, W., Zhang,J., Diehl, T., Levesque, G., Fraser, P., Haass,C., Koo, E.H.M., Seubert,P.,St George-Hyslop, P., Teplow, D.B., Selkoe,D.J. (1997) Presenilin proteins undergo heterogeneous endoproteolysis between thr291 and ala299 and occur as stable N- and C-terminal fragments in normal and Alzheimer brain tissue. Neurobiol. Dis. 3:325-337.

46. Gomez-Isla, T., Wasco, W., Pettingell, W.P., Gurubhagavatula, S., Schmidt, S.D., Jondro, P.D., McNamara, M., Rodes, L.A., DiBlasi, T., Growden W.B., Seubert, P., Schenk, D., Growden, J.H., Hyman, B.T., Tanzi, R.E. (1997) A novel presenilin-1 mutation: increased beta-amyloid and neurofibrillary changes. Ann Neurol. 41:809-813.

47. Galasko,D., Chang, L., Motter, R., Clark, C.M., Kaye, J., Knopman, D., Thomas, R., Kholodenko, D., Schenk, D., Lieberburg, I., Miller, B., Green, R., Basherad, R., Kertiles, L., Boss, M.A., Seubert, P. (1998) High cerebrospinal fluid tau and low amyloid beta42 levels in the clinical diagnosis of Alzheimer disease and relation to apolipoprotein E genotype. Arch Neurol. 55:937-945.

48. Ellis, R.J., Seubert, P., Motter, R., Galasko, D., Deutsch, R., Heaton, R.K., Heyes, M.P., McCutchan, J.A., Atkinson, J.H., Grant, I. (1998) Cerebrospinal fluid tau protein is not elevated in HIV-associated neurologic disease in humans. Neurosci Lett. 254:1-4.

49. Xia, W., Zhang, J., Ostaszewski, B.L., Kimberly, W.T., Seubert, P., Koo, E.H., Shen, J., Selkoe, D.J. (1998) Presenilin 1 regulates the processing of beta-amyloid precursor protein C-terminal fragments and the generation of amyloid beta-protein in endoplasmic reticulum and golgi. Biochemistry. 37:16465-16471.

50. Lasser, R.A., Dukoff, R., Levy, J., Levin, R., Lehtimaki, T., Seubert, P., Sunderland, T. (1998) Apolipoprotein E epsilon 4 allele in association with global cognitive performance and CSF markers in Alzheimer's disease. Int J Gerlar Psychiatry. 13:767-774.

51. Schenk, D., Barbour, R., Dunn, W., Gordon, G., Grajeda, H., Guido, T., Hu, K., Huang, J., Johnson-Wood, K., Khan, K., Kholodenko, D., Lee, M., Liao, Z., Lieberburg, I., Motter, R., Mutter, L., Soriano, F., Shopp, G., Vasquez, N., Vandervert, C., Walker, S., Wogulis, M., Yednock, T., Games, D, Seubert,P. (1999) Immunization with amyloid-beta attenuates Alzheimer-disease-like pathology in the PDAPP mouse. Nature. 400:173-177.

52. Sunderland, T., Wolozin, B., Galasko, D., Levy, J., Dukoff, R., Bahro, M., Lasser, R., Motter, R., Lehtimaki, T., Seubert, P. (1999)

[ps\cv]

Longitudinal stability of CSF tau levels in Alzheimer patients. Biol Psychiatry. 46:750-755.

53. Larson, J., Lynch, G., Games, D., Seubert, P. (1999) Alterations in synaptic transmission and long-term potentiation in hippocampal slices from young and aged PDAPP mice. Brain Res. 840:23-35.

54. Sinha, S., Anderson, J.P., Barbour, R., Basi, G.S., Caccavello, R., Davis, D., Doan, M., Dovey, H.F., Frigon, N., Hong, J., Jacobson-Croak, K., Jewett, N., Keim, P., Knops, J., Lieberburg, I., Power, M., Tan, H., Tatsuno, G., Tung, J., Schenk, D., Seubert, P., Suomensaari, S.M., Wang, S., Walker, D., Zhao, J., McConlogue, L., John, V. (1999) Purification and cloning of amyloid precursor protein beta-secretase from human brain. Nature. 402:537-540.

55. Moriearty, P.L., Seubert, P., Galasko, D., Markwell, S., Unni, L., Vicari, S., Becker, R.E. (1999) Effects of time and cholinesterase inhibitor treatment on multiple cerebrospinal fluid parameters in Alzheimer's disease. Methods Find Exp Clin Pharmacol. 21:549-554.

56. Schenk, D.B., Seubert, P., Lieberburg, I., Wallace, J. (2000) Beta-peptide immunization: a possible new treatment for Alzheimer disease. Arch Neurol. 57:934-936.

57. Bard, F., Cannon, C., Barbour, R., Burke, R.L., Games, D., Grajeda, H., Guido, T., Hu, K., Huang, J., Johnson-Wood, K., Khan, K., Kholodenko, D., Lee, M., Lieberburg, I., Motter, R., Nguyen, M., Soriano, F., Vasquez, N., Weiss, K., Welch, B., Seubert, P., Schenk, D., Yednock, T. (2000) Peripherally administered antibodies against amyloid beta-peptide enter the central nervous system and reduce pathology in a mouse model of Alzheimer disease. Nat Med. 6:916-919.

58. Dovey, H.F., John, V., Anderson, J.P., Chen, L.Z., de Saint Andrieu, P., Fang, L.Y., Freedman, S.B., Folmer, B., Goldbach, E., Holsztynska, E.J., Hu, K.L., Johnson-Wood, K.L., Kennedy, S.L., Kholodenko, D., Knops, J.E., Latimer, L.H., Lee, M., Liao, Z., Lieberburg, I.M., Motter, R.N., Mutter, L.C., Nietz, J., Quinn, K.P., Sacchi, K.L., Seubert, P.A., Shopp, G.M., Thorsett, E.D., Tung, J.S., Wu, J., Yang, S., Yin, C.T., Schenk, D.B., May, P.C., Altstiel, L.D., Bender, M.H., Boggs, L.N., Britton, T.C., Clemens J.C., Czilli, D.L., Dieckman-McGinty, D.K., Droste, J.J., Fuson, K.S., Gitter, B.D., Hyslop, P.A., Johnstone, E.M., Li, W.Y., Little, S.P., Mabry, T.E., Miller, F.D., Audia, J.E. (2001) Functional gamma-secretase inhibitors reduce beta-amyloid peptide levels in brain. J Neurochem. 76:173-181.

59. Games, D., Bard, F., Grajeda, H., Guido, T., Khan, K., Soriano, F., Vasquez, N., Wehner, N., Johnson-Wood, K., Yednock, T., Seubert, P.,

[ps\cv]

Schenk, D. (2000) Prevention and reduction of AD-type pathology in PDAPP mice immunized with Aβ1-42. Ann N Y Acad Sci. 920:274-284.

60. Bacskai, B.J., Kajdasz, S.T., Christie, R.H., Carter, C., Games, D., Seubert, P., Schenk, D, Hyman, B.T. (2001) Imaging of amyloid-beta deposits in brains of living mice permits direct observation of clearance of plaques with immunotherapy. Nat Med. 7:369-372.

61. Brayden, D.J., Templeton, L., McClean, S., Barbour, R., Huang, J., Nguyen, M., Ahern, D., Motter, R., Johnson-Wood, K., Vasquez, N., Schenk, D, Seubert, P. (2001) Encapsulation in biodegradable microparticles enhances serum antibody response to parenterally-delivered beta-amyloid in mice. Vaccine. 19:4185-4193.

62. Schenk, D., Seubert, P., Ciccarelli, R.B. (2001) Immunotherapy with beta-amyloid for Alzheimer's disease: a new frontier. DNA Cell Biol. 20:679-681.

63. Schenk, D., Games, D., Seubert, P. (2001) Potential treatment opportunities for Alzheimer's disease through inhibition of secretases and Aβ immunization. J Mol Neurosci. 22:259-267.

64. Bacskai, B.J., Kajdasz, S.T., McLellan, M.E., Games, D., Seubert, P., Schenk, D., Hyman, B.T. (2002) Non-Fc-mediated mechanisms are involved in clearance of amyloid-beta in vivo by immunotherapy. J Neurosci. 22:7873-7878.

65. Bard, F., Barbour, R., Cannon, C., Carretto, R., Fox, M., Games, D., Guido, T., Hoenow, K., Hu, K., Johnson-Wood, K., Khan, K., Kholodenko, D., Lee, C., Lee, M., Motter, R., Nguyen, M., Reed, A., Schenk, D., Tang, P., Vasquez, N., Seubert, P., Yednock, T. (2003) Epitope and isotype specificities of antibodies to beta-amyloid peptide for protection against Alzheimer's disease-like neuropathology. Proc Natl Acad Sci USA. 100:2023-2028.

66. Bussiere, T., Bard, F., Barbour, R., Grajeda, H., Guido, T., Khan, K., Schenk, D., Games, D., Seubert, P., Buttini. M. (2004) Morphological characterization of Thioflavin-S-positive amyloid plaques in transgenic Alzheimer mice and effect of passive Aβ immunotherapy on their clearance. Am J Pathol. 165:987-995.

67. Schenk, D., Hagen, M., Seubert, P. (2004) Current progress in beta-amyloid immunotherapy. Curr Opin Immunol. 16:599-606.

68. Masliah, E., Hansen, L., Adame, A., Crews, L., Bard, F., Lee, C., Seubert, P., Games, D., Kirby, L., Schenk, D. (2005) Aβ vaccination effects

on plaque pathology in the absence of encephalitis in Alzheimer disease. Neurology. 64:129-131.

69. Malinin, N.L., Wright, S., Seubert, P., Schenk, D., Griswold-Prenner, I. (2005) Amyloid-beta neurotoxicity is mediated by FISH adapter protein and ADAM12 metalloprotease activity. Proc Natl Acad Sci USA. 102:3058-3063.

70. Masliah, E., Rockenstein, E., Adame, A., Alford, M., Crews, L., Hashimoto, M., Seubert, P., Lee, M., Goldstein, J., Chilcote, T., Games, D., Schenk, D. (2005) Effects of alpha-synuclein immunization in a mouse model of Parkinson's disease. Neuron. 46:857-868.

71. Buttini, M., Masliah, E., Barbour, R., Grajeda, H., Motter, R., Johnson-Wood, K., Khan, K., Seubert, P., Freedman, S., Schenk, D., Games, D. (2005) Beta-amyloid immunotherapy prevents synaptic degeneration in a mouse model of Alzheimer's disease. J Neurosci 25:9096-9101.

72. Lee, M., Bard, F., Johnson-Wood, K., Lee, C., Hu, K., Griffith S.G., Black, R.S., Schenk, D., Seubert, P. (2005) Abeta-42 immunization in Alzheimer's disease generates Abeta N-terminal antibodies. Ann Neurol 58:430-435.

[ps\cv]

ABSTRACTS

1. Seubert, P.A., Hoang, L., Renosto, F., and Segal, I.H. (1983) ATP sulfurylase from *Penicillium chrysogenum*: the true specific activity and kinetic mechanism of the enzyme. Annual Meeting of the American Society of Biological Chemists, San Francisco.

2. Seubert, P.A., Baudry, M., Dudek, S., and Lynch, G. (1986) Calmodulin stimulates the degradation of brain spectrin by calpain. Annual Meeting of the Society for Neuroscience, Washington, D.C.

3. Seubert, P., Larson, J., Oliver, M., Jung, M.W., Baudry, M., and Lynch, G. (1988) Stimulation of NMDA receptors induces proteolysis of spectrin in hippocampus. Annual Meeting of the Society for Neuroscience, Toronto.

4. Seubert, P., Lee, K., and Lynch, G. (1989) Cerebral ischemia triggers NMDA receptor-linked cytoskeletal proteolysis of spectrin in hippocampus. Annual Meeting of the Society for Neuroscience, Phoenix.

5. Peterson, C., Vanderklish, P., Seubert, P., Cotman, C., and Lynch, G. (1990) Increased spectrin breakdown in fibroblasts from aged and Alzheimer donors. Annual Meeting of the Society for Neuroscience, St. Louis.

6. Johnson-Wood, K.L., Henriksson, T., Seubert, P., Oltersdorf, T., Lieberburg, I., Schenk, D.B. (1990) Identification of specific binding sites for Iodine-125 secreted APP 751 on intact fibroblast cells. Second International Conference on Alzheimer's Disease and Related Disorders, Toronto.

7. Peterson, C., Vanderklish, P., Seubert, P., Cotman, C., Lynch, G. (1990) Increased spectrin breakdown in fibroblasts from aged and Alzheimer donors. Annual Meeting of the Society for Neuroscience, St. Louis.

8. Sinha, S., Dovey, H.F., Seubert, P. Ward, P.J., Blacher, R.W., Blaber, M., Bradshaw, R.A., Arici, M., Mobley, W.C., Lieberburg, I. (1990) The Kunitz protease inhibitory domain of the beta amyloid precursor protein is sufficient for its protease inhibitory properties. Second International Conference on Alzheimer's disease and Related Disorders, Toronto.

9. Seubert, P., Oltersdorf, T., Lee, M.G., Barbour, R., Blomquist, C., Davis, D.L., Bryant, K., Galasko, D., Thal, L.V., Fritz, L., Lieberburg, I., Schenk, D. β-amyloid precursor protein is processed by an alternative potentially

amyloidogenic pathway. 1992 Annual Meeting of the Society for Neuroscience, Anaheim.

10. Seubert, P., Dovey, H.F., Blacher, R., Varghese, J., Colby, T., Lieberburg, I., Sinha, S. (1992) Identification of a major MET-ASP cleaving peptidase activity from human brain as metalloendopeptidase EC 3.4.24.15. Third International Conference on Alzheimer's Disease and Related Disorders, Abano Terme, Italy.

11. Seubert, P. (1993) Biomarkers of Alzheimer's disease: Beta-amyloid and tau. National Caregiving Foundation Symposium on "Progress in the Diagnosis of Alzheimer's disease," Rancho Mirage.

12. Vigo-Pelfrey, C., Seubert, P., Motter, R., Lieberburg, I., Butler, M., Lee, D., Barbour, R., Schenk, D. (1994) Detection of $A\beta_{1-42}$ in CSF and various cell conditioned media. Annual Meeting of the Society for Neuroscience, Miami Beach.

13. Vigo-Pelfrey, C., Seubert, P., Lee, M., Lieberburg, I., Lee, D., Coria, F., Barbour, R., Schenk, D. (1994) Measurement of tau in human CSF and its possible utility in Alzheimer's disease diagnosis. Fourth International Conference on Alzheimer's Disease and Related Disorders, Minneapolis.

14. Younkin, S.G., Cai, X.-D., Suzuki, N., Cheung, T.T., Greenberg, B., Seubert, P., Lieberburg, I., Golde, T. (1994) Processing of normal and mutant amyloid β protein precursors. Fourth International Conference on Alzheimer's Disease and Related Disorders, Minneapolis.

15. Galasko, D., Hansen, L., Vigo-Pelfrey, C., Schenk, D., Seubert, P. (1995) Antemortem CSF tau is related to neuronal pathology at autopsy in Alzheimer's disease. Annual Meeting of the Society for Neuroscience, San Diego.

16. Haass, C., Lemere, C.A., Capell, A., Citron, M., Seubert, P., Schenk, D., Selkoe, D.J. (1995) β-secretase cleavage of β-amyloid precursor protein with the Swedish mutation occurs within the secretory pathway after the trans-golgi network. Annual Meeting of the Society for Neuroscience, San Diego.

17. McConlogue, L., Johnson-Wood, K., Tan, H., Gordon, M., Dovey, H., Lieberburg, I., Barbour, R., Games, D., Sinha, S., Schenk, D., Seubert, P., Samant, B. (1995) βAPP processing and Aβ production in transgenic mouse brain. Annual Meeting of the Society for Neuroscience, San Diego.

[ps\cv]

18. Litersky, J.M., Seubert, P., Lee, M., Jakes, R., Goedert, M., Johnson, G.V.W. (1995) Tau is phosphorylated by cAMP-dependent protein kinase and calcium/calmodulin-dependent protein kinase II within the microtubule-binding domains at Ser262 and Ser356. Annual Meeting of the Society for Neuroscience, San Diego.

19. Vigo-Pelfrey, C., Motter, R., Kholodenko, D., Barbour, R., Johnson-Wood, K., Galasko, D., Chang, L., Miller, B., Clark, C., Green, R., Olson, D., Southwick, P., Wolfert, R., Munroe, B., Coria, F., Lieberburg, I., Seubert, P., Schenk, D. (1995) CSF levels of $A\beta_{42}$ and tau are altered in Alzheiemr's disease. Annual Meeting of the Society for Neuroscience, San Diego.

20. Sunderland, T., Peterson, R., Zubenko, G., Seubert, P. (1996) Biologic markers in Alzheimer's disease: Potential diagnostic and prognostic tests. Winter Conference on Brain Research, Snowmass.

21. Seubert, P., Motter, R., Schenk, D., Green, R., Chang, L., Miller, B., Clark, C., Galasko, D. (1996) Elevation of CSF tau in early stage Alzheimer's disease. Annual Meeting of the American Academy of Neurology, San Francisco.

22. Johnson-Wood, K., Lee, M., Motter, R., Hu, K., Gordon, G., Barbour, R., Gordon, M., Tan, H., Games, D., Liberburg, I., Schenk, D., Seubert, P., McConlogue, L., (1996) The PDAPP mouse deposits ß-amyloid42 in a region-specific manner similar to Alzheimer's disease. Annual Meeting of the Society for Neuroscience, Washington D.C.

23. Dovey, H.F., Suomensaari, S., de St. Andrieu, P., Barbour, R., Sinha, S., Seubert, P., Schenk, D.B., Lieberburg, I., John, V. (1996) Alzheimer's amyloid precursor processing: Cathepsin D exhibits gamma-secretase activity. Annual Meeting of the Society for Neuroscience, Washington D.C.

24. Diehl, T.S., Citron, M., Gordon, G., Hartley, D., Seubert, P., Selkoe, D.J. (1996) Evidence that Aß42 and Aß40 are generated by different proteases. Annual Meeting of the Society for Neuroscience, Washington D.C.

25. Sunderland, T., Wolozin, B., Galasko, D., Levy, J., Motter, R., Dukoff, R., Bahro, M., Molchan, S., Rubinow, D., Lehtimaki, T., Seubert, P. (1996) Longitudinal stability of CSF tau levels in mid-stage Alzheimer patients. Annual Meeting of the Society for Neuroscience, Washington D.C.

26. Galasko, D.R., Brown, J., Clark, C., Chang, L., Miller, B., Green, R.C., Motter, R., Seubert, P. (1996) CSF tau is increased in very early stages of

Alzheimer's disease. Annual Meeting of the Society for Neuroscience, Washington D.C.

27. Seubert, P., Motter, R., Schenk, D., Lieberburg, I., Kholodenko, D., Galasko, D., Thomas, R., Chang, L., Miller, B., Clark, C., Knopman, D., Kaye, J., Green, R., Kertiles, L., Bashirzadeh, R., Boss, M. (1997) Apo E genotype influences the CSF level of Aß42 in Alzheimer's disease. Annual Meeting of the American Academy of Neurology, Boston, MA.

28. Galasko, D., Seubert, P., Motter, R., Schenk, D., Kholodenko, D., Lieberburg, I., Chang, L., Miller, B., Clark, C., Kaye, J., Camicioli, R., Knopman, D., Green, R., Thomas, R., Kertiles, L., Bashiradeh, R., Boss, M.A. (1997) CSF levels of Aß42 and tau as aids to diagnosing Alzheimer's disease. Annual Meeting of the American Academy of Neurology, Boston, MA.

29. Seubert, P. (1997) CSF levels of tau and Aß42 as diagnostic markers of Alzheimer's disease. International Business Communications Sixth Annual Conference on Alzheimer's Disease, San Francisco, CA.

30. Xia, W., Zhang, J., Ostaszewski, B., Seubert, P., Koo, E., Selkoe, D. (1997) Mutant presenillins increase the generation of the 42-residue amyloid ß peptide in the Golgi apparatus. Annual Meeting of the Society for Neuroscience, New Orleans, La.

31. Ellis, R., Seubert, P., Motter, R., Galasko, D., Heyes, M., Atkinson, J.H., Grant, I. (1997) Cerebrospinal fluid tau protein is not elevated in HIV neurologic disease. Annual Meeting of the Society for Neuroscience, New Orleans, La.

32. May, P.C., Boggs L.N., Calligaro, D., Seubert, P., Johnson-Wood, K., Chen, K., Games, D., Schenk, D., (1997) GFAP as a marker of plaque pathology in the PDAPP transgenic mouse. Annual Meeting of the Society for Neuroscience, New Orleans, La.

[ps\cv]

EXHIBIT B

245

ELSEVIER

Journal of Neuroimmunology 95 (1999) 136–142

Journal of Neuroimmunology

High affinity binding of monoclonal antibodies to the sequential epitope EFRH of β-amyloid peptide is essential for modulation of fibrillar aggregation

D. Frenkel [a,1], M. Balass [b,1], E. Katchalski-Katzir [b], B. Solomon [a,*]

[a] *Department of Molecular Microbiology and Biotechnology, The George S. Wise Faculty of Life Sciences, Tel-Aviv University, Ramat Aviv, Tel-Aviv 69978, Israel*

[b] *Department of Biological Chemistry, The Weizmann Institute of Science, Rehovoth 76100, Israel*

Received 30 September 1998; revised 21 December 1998; accepted 28 December 1998

Abstract

Monoclonal antibodies raised against the N-terminal of Alzheimer's β-amyloid peptide (βAP) were found to modulate its fibrillar aggregation. While mAbs 6C6 and 10D5 inhibit the formation of β-amyloid fibrils, trigger disaggregation and reversal to its non-toxic form, mAb 2H3 is devoid of these properties. MAb 2H3 binds the sequence DAEFRHD, corresponding to position 1–7 of the βAP with high affinity (2×10^{-9}M) similar to its binding with the whole βAP. The EFRH peptide strongly inhibits binding of mAbs 6C6 and 10D5 to βAP, whereas it inhibits weakly the interaction of 2H3 with βAP. Low affinity binding of mAb 2H3 to EFRH might explain its failure in prevention of β-amyloid formation.

Keywords: Antibodies affinity; EFRH epitope; β-Amyloid modulation

1. Introduction

Once released by proteolytic cleavage of amyloid precursor protein (APP) the β-peptide may remain in solution either as a random coil or in a α-helical structure. The transition of the α-helix to β-sheet conformation, with concomitant peptide aggregation, is a proposed mechanism of plaque formation in Alzheimer's disease (Katzman, 1986; Muller-Hill and Beyreuter, 1989; Selkoe, 1991; Ashall and Goate, 1994; Cruz et al., 1997).

The existence of sequences that are kinetically involved in the folding process has previously been suggested in other systems and has been demonstrated by in vitro denaturation–renaturation experiments (Silen and Agard, 1989). Such sequences, which may play a role in the folding pathway, suggest the possibility that they serve not only for the folding process but also may contribute to the conformational stabilization. Monoclonal antibodies (mAbs) which are able to stabilize the conformation of an antigen against incorrect folding may also recognize an incompletely folded epitope and induce native conformation in a partially unfolded protein (Blond and Goldberg, 1987; Solomon and Schwartz, 1995). Appropriate mAbs may interact at such strategic sites where protein unfolding is initiated, thereby stabilizing the protein and preventing further precipitation (Solomon and Balass, 1991; Katzav-Gozansky et al., 1996). Recent studies of β-amyloid fibrils assembled from the synthetic peptide (βAP) showed that mAbs 6C6 and 10D5 raised against the N-terminal region of the βAP (residues 1–28) can disaggregate βA fibrils, restore βAP solubility and prevent neurotoxic effects on PC12 cells (Solomon et al., 1997). The N-terminal epitope of mAb 6C6 and mAb 10D5 within a βAP molecule was found to be a sequential epitope composed of only four amino acid residues (EFRH) located at positions 3–6 of βAP (Frenkel et al., 1998).

The fact that these two mAbs bind with βAP, either when in solution or in an aggregated form, suggests that the N-terminal EFRH epitope is available for the mAbs in both conformations. The inability of mAb 2H3, raised against the N-terminal region 1–12, to modulate fibril aggregation as the above antibodies might be related to

* Corresponding author. Tel.: +972-3-6409711; Fax: +972-3-6409407; E-mail: beka@ccsg.tau.ac.il

[1] The first two authors contributed equally to this work.

0165-5728/99/$ - see front matter
PII: S0165-5728(99)00003-X

different epitope locations or to selective conformational recognition of the peptide.

In order to identify the epitope of mAb 2H3 we employed combinatorial phage display peptide libraries. The construction and application of several epitope libraries, in which different random peptides, the size of 15, 12 or 6 amino acid residues, are expressed on the surface of filamentous phage, has been described (Scott and Smith, 1990; Balass et al., 1993). Identification of the epitope of mAb 2H3, which cannot affect β-amyloid formation despite the fact that it binds to the N-terminal of β-amyloid peptide, may shed light on the importance of specific sequence region, defined as anti-aggregating epitope, on the behavior of the whole βAP molecule.

2. Materials and methods

Synthetic βAP (1–40) was obtained from k-Biological (Rancho Cucamonga, CA, USA). The peptides used were analyzed routinely on HPLC column C18 (Merck, Germany), using a gradient of solvent A:0.1% trifluoroacetic acid in water, and solvent:0.1% trifluoroacetic acid in acetonitrile (70%), water (30%). A linear gradient of 0.1% B to 100% A at room temperature was employed regularly. Purity of the peptides used exceeded 90%.

Monoclonal antibodies, 6C6 and 10D5, raised against soluble fragment of position 1–28 of βAP, and mAb 2H3 raised against a synthetic peptide corresponding to the 1–12 fragment of βAP, were kindly provided by Dr. D. Schenk, Athena Neurosciences (San Francisco, CA, USA) and were used as selectors for the screening of phage-peptide libraries. These mAbs have been extensively characterized (Hyman et al., 1992; Seubert et al., 1992; Games et al., 1995) for their specificity for βAP fragments. The unrelated anti-acetylcholine mAb 5.5 was used as control (Balass et al., 1993).

2.1. Thioflavine T fluorimetric test

Aggregation of β-amyloid peptide βAP (1–40) was measured by the thioflavine (ThT) binding assay, in which the fluorescence intensity reflects the degree of β-amyloid fibrillar aggregation. ThT characteristically stains amyloid-like deposits (Levine, 1993) and exhibits enhanced fluorescence emission of 485 nm and a new excitation peak of 435 nm when added to the suspension of aggregated β-sheet preparations. Aqueous solutions of βAP 0.12 mM (in 0.1 M Tris/HCl pH 7.1) were incubated with mAbs in a ratio of 40:1 (favored to βAP) at 37°C for 1 week. The fluorescence was measured after addition of 1 ml of ThT to the mixture (2 μM in 50 mM Glycine pH 9) using spectrofluorimeter (LSB-50 Perkin Elmer, UK), at the above mentioned wave-lengths.

2.2. Antibody binding to β-amyloid peptide

Binding of antibodies to βAP was analyzed by ELISA, as described previously (Solomon et al., 1993, 1996). To the wells of microtiter plates coated with Eupergit C containing epoxy groups (Rohm, Germany) was added 50 μl βAP (at concentration of 5 ng/μl in KPi, pH 7.5) and incubated overnight at 4°C. Coated plates were washed three times with PBS/0.05% Tween 20 and then were blocked with a mixture of 3% bovine serum albumin and hemoglobin at a ratio of 1:1 (in PBS) for 2 h at 37°C. After washing, the studied antibody was added (1 μg/ml or as otherwise specified) and allowed to bind to the coated plate overnight at 4°C. An alkaline phosphatase-conjugated rabbit anti-mouse immunoglobulin (BioMakor, Rehovot, Israel), diluted at 1:2000, was added to each well and left for 1 h at room temperature. The bound antibody was monitored by the enzymatic activity of alkaline phosphatase, with *p*-nitrophenylphosphate used as a substrate. The color developed was determined spectrophotometrically at 405 nm using an ELISA microtiter plate reader and the constant binding was measured at half maximum binding point.

2.3. Epitope libraries

The 6-mer phage-peptide library used in this study was provided by George P. Smith (University of Missouri, Columbia, MO). The 15-mer phage-peptide library was provided by J.J. Delvin and was constructed by use of the phage M13-derived vector M13LP67, as previously described (Devlin et al., 1990; Scott and Smith, 1990). The phage display peptide library Ph.D-12 was purchased from New England Biolabs (USA). The library consists of $\sim 1.9 \times 10^9$ phage particles (electroporated sequences and comprises a random peptide repertoire of 12 amino acid residues fused to protein III of the M13 phage). Experiments with this library were carried out according to instructions of the manufacturer.

2.4. Biotinylation of antibodies

For antibody biotinylation, 100 μg of each antibody in 0.1 M $NaHCO_3$, pH 8.6, was incubated for 2 h at room temperature with 5 μg of biotinamidocoproate *N*-hydroxy-succinimide ester (Sigma, B 2643) from a stock solution of 1 mg/ml in dimethylformamide and dialyzed at 4°C against phosphate-buffered saline (PBS; 0.14 M NaCl/0.01 M phosphate buffer, pH 7.4) overnight.

2.5. Isolation of phage presenting epitopes from peptide library

A library sample containing 3.8×10^9 infection phage particles was subjected to three rounds of selection (biopanning) and amplification. For each selection cycle a

biotinylated monoclonal antibody (1 μg/μl) in a total volume of 25 μl was used. The phage clones were preincubated with the biotinylated antibody overnight at 4°C, and the reaction mixtures were then layered in 1 ml of PBS containing 0.5% Tween 20 on streptavidin-coated 30 mm polystyrene Petri dishes and incubated for 20 min at room temperature. Unbound phages were removed by extensive washing (10 times for 10 min each) in PBS/0.05% Tween 20. The bound phage was eluted with 0.3 ml of 0.1 M HCl titrated to pH 2.2 with glycine. The eluate was neutralized and used to infect *Escherichia coli* K91 cells. After three rounds of panning individual bacterial colonies containing amplified particles were grown on a microtiter plate and the selected phages were tested by ELISA for their ability to bind to the studied antibody, as described below.

2.6. Antibody binding to isolated phage

Binding of antibodies to phage was analyzed by ELISA. Wells of microtiter plates (Maxisorb, Nunc) were coated with 50 μl (at dilution of 1:1000 in 0.1 M $NaHCO_3$, pH 8.6) of rabbit anti-phage serum and incubated overnight at 4°C. The wells were blocked with a mixture of 3% bovine serum albumin and hemoglobin at the ratio of 1:1 (in PBS) for 2 h at 37°C. Coated plates were washed three times with PBS/0.05% Tween 20, and 50 μl of enriched phage clones containing 10^{10} phage particles were added to the wells and incubated for 1 h at 37°C. After washing, the studied antibody was added (1 μg/ml or as otherwise specified) and allowed to bind to the coated plate overnight at 4°C and the binding constant was measured, as described before. Positive phage clones were propagated and their DNA were sequenced in the insert region at the Sequencing Unit of the Weizmann Institute of Science (Rehovoth, Israel) by using Applied Biosystem Kit (United States, Applied Biosystem).

2.7. Inhibition of antibody binding to β-amyloid peptide

The inhibition of antibody binding to βAP by various small peptides was performed using 250 ng/well β-amyloid peptides (1–40) bound covalently for 16 h at 4°C to ELISA plates that were previously coated with Eupergit-C containing epoxy groups (Rohm, Germany). The plates were washed with PBS/0.05% Tween 20 and blocked with a mixture of 3% bovine serum albumin and hemoglobin, ratio 1:1 (in PBS) for 2 h at 37°C. The peptides were preincubated with each antibody for 30 min at 37°C before their addition to βAP-coated wells and left overnight at 4°C. After washing, bound antibody was detected by incubation with alkaline phosphatase-conjugated rabbit anti-mouse immunoglobulin, as described above. The results were measured in IC_{50}, which is the half molar concentration of peptide that fully inhibits antibody binding.

2.8. Peptides synthesis

Peptides were synthesized by Applied Biosystems Synergy Model 430A in the Unit for Chemical Services of The Weizmann Institute of Science by solid-phase using Fmoc chemistry.

3. Results

3.1. Binding of mAb 2H3 to β-amyloid peptide in comparison to mAbs 6C6 and 10D5

The apparent binding constant of the studied mAbs to βAP were measured by ELISA test, as described, and were found to be of the same order of magnitude, $\approx 10^9$ M^{-1} (data not shown).

3.2. MAb 2H3 does not interfere with the formation of β-amyloid

The fibrillar β-amyloid formation was quantitated by ThT fluorometry binding assay (Levine, 1993). Aliquots of βAP in the absence and/or presence of different mAbs were incubated for a week at 37°C. The ratio of mAb/βAP, 1:40, was found to give maximum quenching of the ThT fluorescence.

Fig. 1 shows that mAb 2H3, at molar ratio βAP/mAb 40:1, did not interfere with fibril aggregation and behaved similarly as the unrelated antibody used as control. MAbs 6C6 and 10D5, at the same βAP/mAb molar ratio, disrupted the fibril structure of β-amyloid with extensive deterioration of fibril morphology, as indicated by a substantial decrease in ThT fluorescence.

3.3. Binding of mAb 2H3 to EFRH-displayed phage

In order to detect whether mAb 2H3 recognizes the EFRH epitope of mAbs 6C6 and 10D5 we used a phage

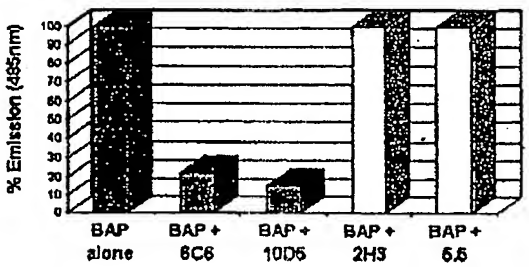

Fig. 1. Interference of mAbs 6C6, 10D5 and 2H3 with fibrillar β-amyloid formation. Estimation of the fluorescence of ThT, which correlates to the amount of fibrillar β-amyloid formed after incubation for a week at 37°C in the presence of mAbs 6C6, 10D5 and 2H3 and unrelated mAb (mAb 5.5 raised against acthylcholine receptor) at molar ratiom 40:1 βAP/mAb using ThT assay, as described.

that bears the hexapeptide YYEFRH. Surprisingly, mAb 2H3 binds to the YYEFRH phage similarly as mAbs 6C6 and 10D5 (Fig. 2).

3.4. Search for epitope of mAb 2H3 using phage peptide libraries

To identify the epitope of mAb 2H3 within βAP, we screened the 6-mer, 12-mer and 15-mer phage-peptide libraries with the biotinylated antibody. In experiments with 6- and 15-mer libraries and biopanning, 90 individual bacterial colonies were isolated following three cycles of biopanning. Each of the isolated colonies was grown in microtiter plates and their phage particles assayed for antibody binding. ELISA analysis revealed that most of the clones bound specifically to mAb 2H3. The DNA of 46 positive clones (25 positive clones from the 6-mer peptide library and 19 from the 15-mer peptide library) were sequenced, and the deduced peptide sequences are shown in Table 1. The sequence EFRH appeared in 12 clones, one additional clone had sequence EDRH with only one residue replacement of aspartic acid with phenylalanine. The consensus sequence for mAb 2H3 selected from a Ph.D-12 mer-peptide library (see Table 2) revealed the epitope, consisting of the following sequence EFRHD corresponding to the N-terminal region of β-amyloid peptide at position 3–7.

3.5. Competition between βAP and various synthetic peptides for antibody binding

The interaction of mAb 2H3 with βAP was further assayed by competitive inhibition experiments. Fig. 3 shows that the synthetic peptide EFRH, which bears the epitope of mAbs 6C6 and 10D5, inhibits binding of mAb 2H3 to βAP with an IC_{50} value of only 3×10^{-4} M, while the synthetic peptide EFRHD, which was implied by the phage-epitope library, inhibits binding of mAb 2H3 to βAP with an IC_{50} value of 2×10^{-6} M. In order to clarify whether EFRHD is the whole epitope of mAb 2H3 within βAP, we synthesized peptides derived from βAP (that include the sequence EFRHD) such as: AEFRHD (residues at position 2–7), DAEFRHD (residues at position 1–7), DAEFRHDSG (residues at position 1–9), and βAP itself (residues at position 1–40). As shown in Fig. 3, the synthetic peptide DAEFRHD corresponding to position 1–7 inhibits binding of mAb 2H3 to the βAP with an IC_{50} value of about 2×10^{-9} M, similar to βAP 1–40. Fig. 3 and Table 3 show the importance of aspartic acid (D) at

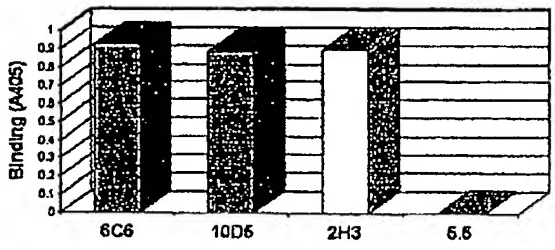

Fig. 2. Binding of mAbs 6C6, 10D5 and 2H3 to YYEFRH-phage. Unrelated mAb 5.5 raised against acethylcoline receptor was used as control. Antibodies were added to the phage-coated wells and binding was analyzed by ELISA, as described.

Table 1
Sequences of peptide-presenting phage selected by mAb 2H3

	Sequence	No. of phage
A	YYEFRH	5
	FTEFRH	5
	FNEFRH	1
	EFDHAG	1
	GAWPDLLEFRHSFGR EFDHAG	1
B	LFRHFN	1
	PLFRHN	1
	LFRHGN	1
	LFRHSVFPGSRGWCC	1
	GSLFRHSQLLPAVLR	1
	SARPSESSLFRHELG	2
	LFRHGN	1
	GYFRHN	1
	PYFRHI	1
	VVDSTTGIRIFYFRH	1
	HDVDYFRHPPEVSLL	1
	PAFAFGSLALSFFRH	1
	PSHRLSSRIFFRHSP	2
	FFRPER	1
	AISDPFFRPERMRVD	2
	NIWFRH	3
	PLDFRH	1
	NIGFRH	1
	PLDFRH	1
	GAADFDFRHGRAVT	1
C	HHLFXLGLKWRVRHD	5
	VIWARHDLLFPYDNH	2
	QKVWLIGYGRHDRLF	1
	LFDRHD	1
	FHSIPVMRTSWFRHD	1
	PMFRHD	1

β-Amyloid 1–9: DAEFRHDSG.

Table 2
Epitopes for mAb 2H3 selected from Ph.D 12-mer peptide library

Sequence	No. of phage
DDLFRHMPQTLA	2
HHTNDSYFRHTP	1
NPQHREFRHYVY	1
TTLSEFRHQWTP	1
SYTEFRHNILPM	1
HEFRHYDAKVTW	1
SEFRHDLNVPPA	1

β-Amyloid 1–12: DAEFRHDSGYEV.

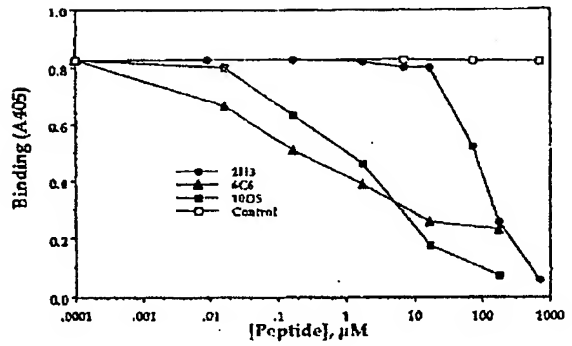

Fig. 3. Inhibition of mAb 2H3 or mAb 6C6 or mAb 10D5 binding to βAP by the synthetic peptide EFRH. The assay was done using 1 μg/ml of each mAb per βAP-coated well and increased concentrations of peptide, as previously described.

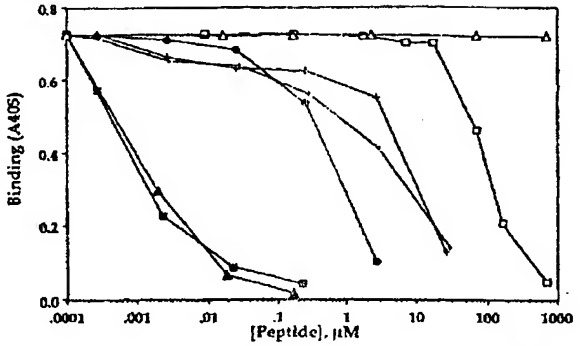

Fig. 4. Inhibition of mAb 2H3 binding to βAP by the synthetic peptides derived from N-terminal 1–12 of β-amyloid peptide. The assay was done as described with 1 μg/ml of each mAb per βAP-coated well and increased concentrations of each peptide. The peptide WVLD was used as a control. (– Δ –), – □ – EFRH; – × –, AEFRH; – + –, EFRHD; – • –, DAEFRH; – ■ –, DAEFRHD.

position 1 of βAP, which added three orders of magnitude to a IC_{50} value of EFRHD, which was implied by the phage-peptide library alone (2×10^{-6} M) and five orders of magnitude to the IC_{50} value of synthetic peptide EFRH (3×10^{-4} M), as shown in Fig. 4. The peptide DAEFRH inhibited mAb 2H3 binding to βAP with an IC_{50} value of only 2×10^{-7} M, indicating the importance of aspartic acid (D) in position 7 of the epitope of mAb 2H3 within the βAP (Table 2). Comparison between the IC_{50} value of the peptide AEFRHD (5×10^{-6} M) and the IC_{50} value of the peptide EFRHD (2×10^{-6} M) suggested that amino acid alanine is not vital to the epitope of mAb 2H3. These data and the data listed in Table 2 indicate that the epitope of mAb 2H3 within the βAP molecule **DXEFRHD** is an epitope composed of seven amino acid residues corresponding to positions 1–7 in the βAP.

3.6. Comparison between the affinity binding of mAbs 2H3, 6C6 and 10D5 to the synthetic peptide EFRH

In order to learn the difference between the epitopes of the three mAbs we used a series of synthetic peptides containing the EFRH core as competitors in the binding of each mAb to the βAP. While EFRH inhibits the binding of mAbs 6C6 and 10D5 to βAP with an IC_{50} value of about 10^{-7} M, it inhibits mAb 2H3 with an IC_{50} value of only about 10^{-4} M (Fig. 4). Table 3 shows that the synthetic peptide DAEFRHD inhibits the binding of mAbs 6C6 and 10D5 to the βAP with an IC_{50} value of about 10^{-7} M (like the peptide EFRH), but it strongly inhibits the binding of mAb 2H3 to the βAP with an IC_{50} value of about 10^{-9} M.

Table 3
Inhibition of mAbs 2H3, 6C6 and 10D5 binding to βAP (IC_{50}) value by peptides corresponding to the N-terminus of βAP molecule

Peptide	mAb 2H3	mAb 6C6	mAb 10D5
EFRH (3–6)	3.0×10^{-4} M	1.0×10^{-7} M	3.4×10^{-6} M
DAEFRH (1–6)	2.0×10^{-7} M	6.0×10^{-7} M	1.5×10^{-7} M
EFRHD (4–7)	2.0×10^{-6} M	5.0×10^{-7} M	1.5×10^{-6} M
AEFRHD (2–7)	5.0×10^{-6} M	7.0×10^{-7} M	8.0×10^{-7} M
DAEFRHD (1–7)	2.0×10^{-9} M	2.0×10^{-7} M	1.5×10^{-7} M
DAEFRHDSG (1–9)	2.0×10^{-9} M	4.0×10^{-7} M	7.8×10^{-7} M
βAP (1–40)	3.0×10^{-9} M	4.0×10^{-7} M	4.2×10^{-7} M
DA**DMKYDSG**[a]	Nd[b]	Nd[b]	Nd[b]

[a] Control peptide corresponding to positions 1–9 in βAP where four substitutions represented by bold underlined print were carried out.
[b] IC_{50} value of less than 10^{-2} M which cannot be detected by ELISA assay.

4. Discussion

Recent studies showed that site-directed mAbs towards the N-terminal region of the β-amyloid peptide can bind to β-amyloid fibrils, leading to their disaggregation and inhibition of their neurotoxic effect (Solomon et al., 1996). The involvement of the N-terminal region in the conformational transformations of βAP was previously confirmed by a number of authors in studies using synthetic peptides bearing the βAP sequence in various experimental conditions (Lorenzo and Yankner, 1994; Howlett et al., 1995; Kirshenbaum and Daggett, 1995; Lee et al., 1995; Soto et al., 1995). It was found that the amino acid residues 1–9 contribute mainly to the solubility of βAP as they were assumed to be located at the filament surface, mediating interactions between individual filaments. In vivo, this amino acid residue region could also be involved in the binding of other proteins that are found in amyloid deposits.

As shown previously, the immunocomplex of βAP with the selected mAbs can prevent β-amyloid peptide aggregation (Solomon et al., 1996). In an earlier report (Frenkel et al., 1998) we defined the N-terminal anti-aggregation epitope of mAbs 6C6 and 10D5 as a sequential epitope

composed of only four amino acid residues (EFRH) located at position 3–6 within βAP. The localization of this epitope may lead to the assumption that every mAb that binds to the same epitope within the βAP has the capability to interfere with β-amyloid formation. However, mAb 2H3, raised against a peptide containing the first 1–12 residues of the βAP, which also recognizes EFRH, showed a considerably lower effect on the prevention of in vitro β-amyloid formation and on the disruption of the β-amyloid already formed (Hanan-Aharon and Solomon, 1996). In this connection, it is pertinent to note that in spite of the incapability of 2H3 to modulate βAP aggregation it binds strongly to the phage bearing the hexapeptide YYEFRH which displays the epitope EFRH of mAb 6C6 and 10D5 (Fig. 2).

Using three different types of phage-peptide libraries displaying 6-mer, 12-mer or 15-mer (Devlin et al., 1990; Scott, 1992) we identified four types of consensus sequences that bind to mAb 2H3, among them EFRH, FRH, FRHD, RHD (Table 1) and EFRHD (Table 2). The EFRH peptide, which consists of the epitope of mAbs 6C6 and 10D5, inhibits binding of 2H3 to βAP with a lower affinity of 10^{-4} M (Fig. 3) emphasizing that this sequence does not represent the whole epitope of mAb 2H3. The synthetic peptides corresponding to positions 1–7 and 1–40 βAP inhibit binding of mAb 2H3 to βAP with the same value of IC_{50} of about 10^{-9} M (Table 3). These peptides clearly define the sequence of DAEFRHD, corresponding to position 1–7 of the βAP, as the epitope that contains all the elements necessary for maximum binding of mAb 2H3 to the βAP molecule. Comparison between the IC_{50} value of peptide AEFRHD (5×10^{-6} M) to the IC_{50} value of peptide EFRHD (2×10^{-6} M) shows that in the epitope of mAb 2H3 the amino acid alanine in position 2 within βAP is not essential, and the real epitope is the sequential epitope DXEFRHD (Tables 2 and 3).

These data revealed that even though the epitope of mAbs 6C6 and 10D5 (EFRH) represents partly the epitope of mAb 2H3 (DXEFRHD) the latter is devoid of the capability to interfere with the fibril formation of β-amyloid. We assume that the EFRH epitope is involved in modulation of the aggregation process, and acts as a regulatory site controlling both the solubilization and the disaggregation process of the βAP molecule. We found that while EFRH strongly inhibits binding of mAbs 6C6 and 10D5 to βAP (10^{-7} M), it weakly inhibits binding of mAb 2H3 to βAP (10^{-4} M). Binding of mAbs with a high affinity to this EFRH region prevents aggregation of the βAP while mAbs showing a low affinity to this epitope did not prevent aggregation.

The tendency of βAP to adopt different conformations, such as soluble α-helix and/or β-sheet, involves the N-terminal of the peptide. Therefore, while mAbs 6C6 and 10D5 bind to epitope EFRH when the β-amyloid peptide is either in solution or in an aggregate form, mAb 2H3 seems to bind to the sequential epitope DXEFRHD, which might be available only in soluble conformation of βAP.

We can conclude that the failure of mAb 2H3 to prevent aggregation is attributed to the low binding constant of this mAb with the EFRH sequence of βAP. We further assume that the epitope EFRH, which is located at the soluble tail of the N-terminal region, is involved in the aggregation process and acts as a regulatory site controlling both the solubilization and the disaggregation process of the Aβ molecule. The experimental findings with mAb 2H3 show clearly that the epitope of this antibody DXEFRHD is larger than that of mAbs 6C6 and 10D5 that recognize a part of this epitope, EFRH. Aggregation of βAP leads to a conformation change in the epitope of 2H3, with concomitant hiding of the essential residues characterizing the epitope of this antibody. Future structural work using X-ray and crystallography can emphasize the importance of these residues as well as the corresponding critical residues in the variable region of those mAbs involved in antibody:antigen immunocomplex. This study can provide the foundation for potential therapeutic approaches targeted at fibrillar β-amyloid accumulation in Alzheimer disease.

There are several conformational diseases where the normal production of a soluble protein is affected by various factors which lead to amyloid formation (Strittmatter et al., 1996; Dalal et al., 1997; Lomas and Carrell, 1997). Finding their 'aggregation epitope' and preparation of antibodies against this region may modulate and prevent their aggregation.

Acknowledgements

We would like to express our thanks to Dr. Dale Schenk of Athena Neuroscience for his generosity in supplying monoclonal antibodies. This work was supported with a donation from the Kipp Foundation and a grant from the Center for the Study of Emerging Diseases.

References

Ashall, F., Goate, A.M., 1994. Role of the β-amyloid precursor protein in Alzheimer disease. Trends Biochem. Sci. 19, 42–46.

Balass, M., Heldman, Y., Cabilly, S., Givol, D., Katchalski-Katzir, E., Fuchs, S., 1993. Identification of a hexapeptide that mimics a conformation-dependent binding site of acetylcholine receptor by use of a phage-epitope library. Proc. Natl. Acad. Sci. U.S.A. 90, 10638–10642.

Blond, S., Goldberg, M., 1987. Partly native epitopes are already present on early intermediates in the folding of tryptophan synthase. Prof. Natl. Acad. Sci. U.S.A. 84, 1147.

Cruz, L., Urbane, B., Buldyrev, S.V., Christie, R., Gomez-Isla, T., Havlin, S., McNamara, M., Stanley, H.E., Hyman, B.T., 1997. Aggregation and disaggregation of senile plaques in Alzheimer's disease. Proc. Natl. Acad. Sci. U.S.A. 94, 7612–7616.

Dalal, S., Balasubramanian, S., Regan, L., 1997. Protein alchemy: changing β-sheet into α-helix. Nature Struc. Biol. 4, 548–552.

Devlin, J.J., Panganiban, L.C., Devlin, P.E., 1990. Random peptide

libraries: a source of specific protein binding molecules. Science 249, 404–406.

Frenkel, D., Balass, M., Solomon, B., 1998. N-Terminal EFRH sequence of Alzheimer's β-amyloid peptide represents the epitope of its anti-aggregation antibodies. J. Neuroimmunol. 88, 85–90.

Games, D., Adams, D., Alessandrini, R., Barbour, R., Berthelette, P., Blackwell, C. et al., 1995. Alzheimer-type neuropathology in transgenic mice overexpressing V717F β-amyloid precursor protein. Nature 373, 523.

Hanan-Aharon, E., Solomon, B., 1996. Inhibitory effect of monoclonal antibodies on Alzheimer's β-amyloid peptide aggregation. Amyloid: Int. J. Exp. Clin. Invest. 3, 130–133.

Howlett, D.R., Jennings, K.H., Lee, D.C., Clark, M.S.G., Brown, F., Wetzel, R., Wood, S.J., Camilleri, P., Roberts, G.W., 1995. Aggregation state and neurotoxic properties of Alzheimer Beta-amyloid peptide. Neurodegeneration 4, 23–32.

Hyman, B.T., Tanzi, R.B., Marxloff, K., Barbour, R., Schenk, D.B., 1992. Kunitz protease inhibitor-containing amyloid β-protein precursor immunoreactivity in Alzheimer's disease. J. Neuropath. Exp. Neurol. 51, 76.

Katzav-Gozansky, T., Hanan, E., Solomon, B., 1996. Effect of monoclonal antibodies in preventing carboxypeptidase A aggregation. Biotechnol. Appl. Biochem. 23, 227.

Katzman, R., 1986. Alzheimer's disease. N. Engl. J. Med. 314, 964–973.

Kirshenbaum, K., Daggett, V., 1995. Sequence effects on the conformational properties of the amyloid β (1–28) peptide: testing a proposed mechanism for the α → β transition. Biochemistry 34, 7640–7647.

Lee, J.P., Stimson, E.R., Ghilardi, J.R., Mantyh, P.W., Lu, Y.-A., Felix, A.F., Llanos, W., Behbin, A., Cummings, M., van Criekinge, M., Timms, W., Maggio, J.E. et al., 1995. HNMR of Aβ amyloid peptide congeners in water solution. Conformational changes correlate with plaque competence. Biochemistry 34, 5191–5200.

Levine, H. III, 1993. Thioflavine T interaction with synthetic Alzheimer's disease β-amyloid peptides: detection of amyloid aggregation in solution. Protein Sci. 2, 404–410.

Lomas, D.A., Carrell, R.W., 1997. Conformational disease. Lancet 350, 134–138.

Lorenzo, A., Yankner, B.A., 1994. β-Amyloid neurotoxicity requires fibril formation and is inhibited by Congo red. Proc. Natl. Acad. Sci. U.S.A. 91, 12243–12247.

Muller-Hill, B., Beyreuter, K., 1989. Molecular biology of Alzheimer's disease. Annu. Rev. Biochem. 58, 287–307.

Seubert, P., Vigo-Pelfrey, C., Esch, F., Lee, M., Dovey, H., Davis, D., Sinha, S., Schlossmacher, M., Whaley, J., Swindlehurst, C., McCormack, R., Wolfert, R., Selkoe, D., Lieberburg, I., Schenk, D., 1992. Isolation and quantification of soluble Alzheimer's β-peptide from biological fluids. Nature 359, 325.

Scott, J.K., 1992. Discovering peptide ligands using epitope libraries. Trends Biochem. Sci., 241–245.

Scott, J.K., Smith, G.P., 1990. Searching for peptide ligands with an epitope library. Science 249, 386–390.

Selkoe, D.J., 1991. The molecular pathology of Alzheimer disease. Neuron 6, 487–498.

Silen, J.L., Agard, D.A., 1989. The α-lytic protease pro-region does not require a physical linkage to activate the protease domain in vivo. Nature 341, 462.

Solomon, B., Balas, N., 1991. Thermostabilization of carboxypeptidase A by interaction with its monoclonal antibodies. Biotechnol. Appl. Biochem. 14, 202.

Solomon, B., Schwartz, F., 1995. Chaperone-like effect of monoclonal antibodies on refolding of heat-denatured carboxypeptidase A. J. Molec. Recogn. 8, 72.

Solomon, B., Schmitt, S., Schwartz, F., Levi, A., Fleminger, G., 1993. Eupergit C-coated membranes as solid support for a sensitive immunoassay of human albumin. J. Immunol. Meth. 157, 209.

Solomon, B., Koppel, R., Hanan, E., Katzav, T., 1996. Monoclonal antibodies inhibit in vitro fibrillar aggregation of the Alzheimer β-amyloid peptide. Proc. Natl. Acad. Sci. U.S.A. 93, 452–455.

Solomon, B., Koppel, R., Frenkel, D., Hanan-Aharon, E., 1997. Disaggregation of Alzheimer β-amyloid by site-directed mAb. Proc. Natl. Acad. Sci. U.S.A. 94, 4109–4112.

Soto, C., Castano, E.M., Frangione, B., Inestrosa, N.C., 1995. The α-helical to β-strand transition in the amino-terminal fragment of the amyloid β-peptide modulates amyloid formation. J. Biol. Chem. 270, 3063–3067.

Strittmatter, W.J., Burke, J.R., DeSerrano, V.S., Huang, D.Y., Matthew, W., Saunders, A.M., Scott, B.L., Vance, J.M., Weisgraber, K.H., Roses, A.D., 1996. Protein–protein interactions in Alzheimer's disease and the CAG triplet repeat diseases. Cold Spring Harbor Symposia on Quantitative Biology LXI, 597–605.

EXHIBIT C

THE JOURNAL OF BIOLOGICAL CHEMISTRY
Vol. 270, No. 7, Issue of February 17, pp. 3063–3067, 1995
Printed in U.S.A.

The α-Helical to β-Strand Transition in the Amino-terminal Fragment of the Amyloid β-Peptide Modulates Amyloid Formation*

(Received for publication, November 1, 1994)

Claudio Soto‡, Eduardo M. Castaño§, Blas Frangione§, and Nibaldo C. Inestrosa¶

From the Departamento de Biología Celular y Molecular, Facultad de Ciencias Biológicas, Pontificia Universidad Católica de Chile, Santiago, Chile and the §Department of Pathology, New York University, Medical Center, New York, New York 10016

Amyloid-β peptide (Aβ) consists of a hydrophobic C-terminal domain (residues 29–42) that adopts β-strand conformation and an N-terminal domain (amino acids 10–24) whose sequence permits the existence of a dynamic equilibrium between an α-helix and a β-strand. In this paper we analyzed the effect of the alternate N-terminal conformations on amyloid fibril formation through the study of the analogous Aβ peptides containing single amino acidic substitutions. The single mutation of valine 18 to alanine induces a significant increment of the α-helical content of Aβ, determined by Fourier transform infrared spectroscopy and circular dichroism and dramatically diminishes fibrillogenesis, measured by turbidity, thioflavine T binding, Congo red staining, and electron microscopic examination. In hereditary Dutch cerebral hemorrhage with amyloidosis (a variant of Alzheimer's disease), the substitution of glutamine for glutamic acid at position 22 decreased the propensity of the Aβ N-terminal domain to adopt an α-helical structure, with a concomitant increase in amyloid formation. We propose that Aβ exists in an equilibrium between two species: one "able" and another "unable" to form amyloid, depending on the secondary structure adopted by the N-terminal domain. Thus, manipulation of the Aβ secondary structure with therapeutical compounds that promote the α-helical conformation may provides a tool to control the amyloid deposition observed in Alzheimer's disease patients.

Alzheimer's disease (AD)[1] is the most common form of dementia in adults. AD is characterized neuropathologically by amyloid deposition in the form of neuritic plaques and congophilic angiopathy as well as by the formation of neurofibrillary tangles (1). The main component of amyloid is the 4.3-kDa amyloid β-peptide (Aβ), which is part of a much longer precursor protein (APP) codified in chromosome 21 (2).

Amino acid sequence analyses of the Aβ peptide by the Chou-Fasman (3) and Garnier-Osguthorpe-Robson (4) methods indicate that the probability of finding β-strand conformation in Aβ is high within the C-terminal region after residue 28. The region between amino acids 10 and 24 presents a high and similar probability to display α-helix or β-strand conformation (5). There are also two probable β-turns between residues 6 and 8 and between residues 24 and 29. Using synthetic peptides and spectroscopic techniques, the secondary structure assignments obtained by predictive methods have been confirmed (6–9).

While the hydrophobic segment in the C-terminal domain of Aβ invariably adopts a β-strand structure in aqueous solutions, independently of pH or temperature conditions, the N-terminal domain can show different conformations and solubilities depending on environmental conditions (8–10). In fact, the N-terminal domain exists as a soluble monomeric α-helical structure at pH 1–4 and pH greater than 7. However, at pH 4–7 it rapidly precipitates into an oligomeric β-sheet structure. Furthermore, it adopts an α-helical conformation in a membrane-mimicking solvent that promotes intramolecular hydrogen bonding (8). Thus, Aβ exists in two alternative conformations depending on the secondary structure adopted by the N-terminal domain. These alternative conformations have different solubility properties and may determine changes in the rate of amyloid fibril formation. We had hypothetized that the structure adopted by the N-terminal domain of Aβ is important in amyloid fibril formation (5). In the present work we have evaluated this possibility by analyzing the ability of Aβ sequences containing single mutations in its N-terminal domain to form amyloid fibrils. Specifically we studied amyloid formation using peptides containing the mutation of valine to alanine at residue 18, and glutamic acid to glutamine at position 22 (Dutch variant of Aβ).

EXPERIMENTAL PROCEDURES

Predicted Secondary Structure—The α-helix, β-sheet, and β-turn propensities for different sequences of Aβ peptide were calculated by the Chou and Fasman secondary structure prediction algorithm (3), using the program Protyle version 3.01 from Copyright.

Peptide Synthesis and Characterization—Fragment 1–40 of the Aβ wild-type peptide (SP40) was obtained from Sigma. Peptide 1–40, containing a valine to alanine mutation in position 18 (SP40A), was synthesized by Chiron Corp. Inc., Emeryville, CA. The Dutch variant of Aβ (SP40Q) was synthesized by using solid-phase techniques at the Center for the Analysis and Synthesis of Macromolecules, State University of New York, Stony Brook, NY. All peptides were purified by reverse-phase high performance liquid chromatography, and their purity was evaluated by amino acid sequence analysis.

Preparation of the Peptide Samples—Stock solutions of the peptides were prepared by dissolving them in 50% acetonitrile. The concentration of the stock solution was determined by amino acid composition analysis on a Waters Pico-Tag amino acid analyzer, after hydrolyzing the samples under reduced pressure in the presence of 6 M HCl for 20 h at 110 °C. Next, peptide aliquots were lyophilyzed and resuspended in the buffer used in the aggregation or amyloid detection assay.

Fourier Transform Infrared Spectroscopy—IR spectra were collected

* This work was supported in part by grants from FONDECYT (Grant 1940694 to N. C. I. and Grant 3930010/93 to C. S.), Sandoz Foundation for Gerontological Research (to C. S.), and National Institutes of Health Grants AG10953 and AG05891 (to B. F.). The costs of publication of this article were defrayed in part by the payment of page charges. This article must therefore be hereby marked "*advertisement*" in accordance with 18 U.S.C. Section 1734 solely to indicate this fact.

‡ Recipient of a postdoctoral fellowship from Fundación Andes de Chile.

¶ To whom correspondence should be addressed: Molecular Neurobiology Unit, Catholic University of Chile, P. O. Box 114-D, Santiago, Chile. Fax: 56-2-2225515.

[1] The abbreviations used are: AD, Alzheimer's disease; Aβ, amyloid β-peptide; APP, amyloid precursor protein; ThT, thioflavine T; FT-IR, Fourier transform infrared spectroscopy; TFE, 2,2,2-trifluorethanol.

in a Perkin-Elmer System 2000 FT-IR operated at 2 cm^{-1} resolution. The peptide solutions (20 mg/ml) were prepared in 25 mM HEPES dissolved in ^2H_2O, pD 7.5. Electrode readings were uncorrected for deuterium effects. Sample aliquots (20 μl) were placed in demountable cells containing CaF_2 windows separated by 50-μm Teflon spacers. The trifluoroacetic acid (used in high performance liquid chromatography purification of the peptides) was removed as described by Fraser *et al.* (11).

Circular Dichroism Measurements—CD spectra were obtained with a Jasco spectropolarimeter, model J-720 at room temperature in a 0.1-cm path-length cell. Double distilled and deionized water and TFE (spectroscopy grade) were used as solvents. Spectra were recorded at 1-nm intervals over the wavelength range 180 to 260 nm. Results are expressed in terms of molar ellipticity (θ) in units of degrees cm^2 $dmol^{-1}$. All the spectra were obtained by subtracting buffer base-line spectra and smoothed by using the algorithm provided by Jasco. The approximate percent of α-helical content was determined using the 208 nm absorption (12) according to the following equation: % α-helix = $([\theta]_{208} - 4000/-33000 - 4000) \times 100$.

Aggregation Studies—Lyophilized aliquots of the peptides were resuspended in 0.1 M sodium acetate, pH 5.0. At various times, the aggregation was detected via turbidity measurements at 405 nm as described previously by Jarrett *et al.* (13).

Amyloid Detection in Suspension—Amyloid quantification in suspension was performed by the thioflavine T method (14, 15), with a few modifications. In short, 1.5 μM thioflavine T (ThT) in a buffer of 50 mM glycine, pH 9.5, was added to peptide aliquots previously incubated in 0.1 M Tris-HCl, pH 7.5. Immediately thereafter, the fluorescence was monitored at excitation 435 nm and emission 490 nm on a Hitachi 200 spectrofluorometer. A time scan of fluorescence was performed, and three values after the decay reached a plateau (280, 290, and 300 s) were averaged after subtracting the background fluorescence of 1.5 μM ThT. The mean ± standard deviation for three separated experiments made in duplicated is shown in Figs. 2*B* and 4*B*.

Congo Red Staining—Amyloid detection by Congo red was performed as described previously (16).

Electron Microscopy—For fibril formation, the peptides (1–2 mg/ml) were incubated in phosphate-buffered saline for 5 days at room temperature. The 300-mesh Formvar-coated nickel grids were floated on the peptide solutions, air-dried, and negatively stained with uranyl acetate. The specimens were viewed with a Philips EM-300 electron microscope at 100 kV.

RESULTS

To study the relation between the secondary structure of Aβ and its ability to form amyloid fibers, we designed a mutation that does not produce a significant change in the ionic or hydrophobic properties of Aβ but is sufficient to increase the propensity of the N-terminal domain of Aβ to adopt the α-helical conformation. A peptide in which valine at position 18 of Aβ was replaced by alanine (SP40A) was synthesized. This modification considers that valine at position 18 is the residue that has the highest probability value to exist as a β-strand in the N-terminal region of Aβ. Valine is an amino acid that destabilizes the α-helix, whereas alanine is a very good helix-former in aqueous solution. The above statement is supported by thermodynamic considerations (17–19), by comparative studies of the helix-forming tendency in synthetic peptides (20), and by statistical surveys (3, 4). In fact, by comparative analysis of the secondary structure of both peptides through FT-IR, we found that the modified peptide contains a significant amount of α-helical structure (Fig. 1*A*). A quantitative analysis of the spectra gave the following percentage of secondary structure for SP40A: 32.8% of α-helix, 31.3% of β-sheet, 24.7% of random coil, and 11.2% of β-turn, while the percentage of secondary structure for the control peptide, containing the 1–40 sequence of Aβ (SP40), was: 1.1% of α-helix, 60.4% of β-sheet, 31.4% of random coil, and 7.1% of β-turn. The higher content of α-helix in the modified peptide was additionally found through CD studies in the presence of 20% TFE (Fig. 1*B*). The α-helical content for SP40 and SP40A in this solvent was 16.6% and 40.9%, respectively. The higher level of α-helix obtained in the last experiment may be due to the presence of TFE, which is a solvent that stabilizes the α-helical conformation (21).

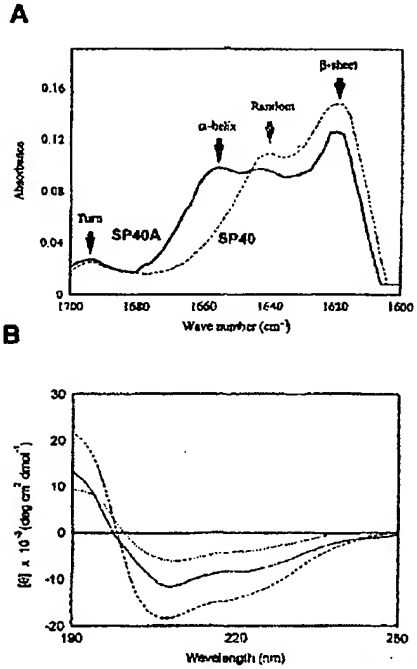

FIG. 1. **Fourier transform infrared and Circular dichroism studies of wild type and mutant Aβ peptides.** In *A* is shown the FT-IR spectra taken under the following conditions; peptide aliquots of 20 mg/ml (20 μl) prepared in 25 mM HEPES (disolved in ^2H_2O), pD 7.5, were placed in CaF_2 cells and the spectra were collected at 2 cm^{-1} of resolution taking 500 scans. The spectra obtained with SP40 (*dashed line*) and SP40A (*solid line*) are shown. The *arrows* indicate the position of the band in the amide I region corresponding to the α-helix (~1653 cm^{-1}), β-sheet (~1626 cm^{-1}), β-turn (~1696 cm^{-1}), and random coil (~1644 cm^{-1}) structures. In *B* the CD spectra of SP40 (*solid line*), SP40A (*dashed line*), and SP40Q (*dotted line*) is shown. Aliquots of peptides were disolved in 20% TFE prepared in 10 mM sodium phosphate, pH 7.4. The peptide concentration was 0.15 mg/ml in a final volume of 0.3 ml. The spectra were recorded at room temperature as described under "Experimental Procedures."

The comparative study of the solubility properties of SP40 and SP40A was performed by means of turbidimetric measurements. After 48 h of incubation, SP40A became aggregated to a lesser extent than SP40 at equal concentration (Fig. 2*A*). Thus, at a peptide concentration of 4.0 mg/ml, SP40A exhibits 80% less aggregation than the control. However, an increase in the turbidity indicates only aggregation, but not necessarily amyloid formation. To semi-quantify the amount of amyloid formed under each condition, we used a novel method based on the fluorescence emission by thioflavine T (ThT) bound to amyloid (14, 15). ThT binds specifically to amyloid and this binding produces a shift in the emission spectra and a fluorescence enhancement proportional to the amount of the amyloid formed (15). The ability to form amyloid, measured by the ThT method, was compared between SP40 and SP40A. The modified peptide showed very little fluorescence in comparison with SP40 at a concentration of 1 mg/ml (Fig. 2*B*). To further evaluate the ability of SP40A to form amyloid, we performed staining with Congo red. Light microscopic examination after Congo red staining showed that only SP40 (1 mg/ml), incubated 5 days, displayed a significant green birefringence under polarized light, while the modified peptide exhibited only a slight green birefringence under the same conditions (data not shown). Furthermore, the presence and the morphology of the fibrils formed by both peptides was studied by electron microscopy.

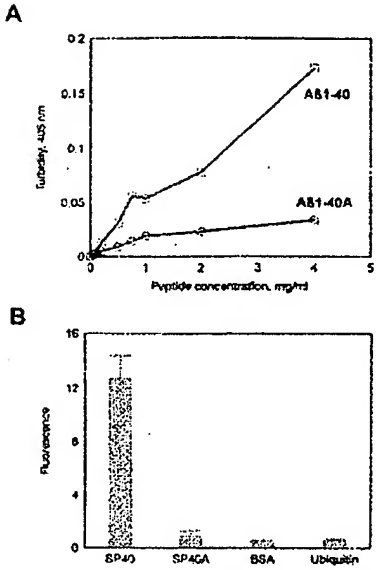

FIG. 2. **Aggregation and amyloid formation by SP40 and SP40A.** The aggregation level obtained with different concentrations of SP40 (*squares*) and SP40A (*circles*) was studied (*A*). The peptides were incubated for 48 h at 25 °C in 0.1 M sodium acetate buffer, pH 5.0, at various peptide concentrations, from 1 μg/ml to 4 mg/ml. The aggregation was measured by the turbidity at 405 nm, as described in "Experimental Procedures". The value shown represent the mean between 2 different experiments. The amyloid formation was quantified through the ThT method (*B*). Aliquots of each peptide in a concentration of 1 mg/ml (0.25 mM) were incubated for 15 h in 0.1 M Tris-HCl, pH 7.5, at room temperature. Then the amyloid formation was quantified as described under "Experimental Procedures". The protein concentration for BSA and ubiquitin was 1 mg/ml. The graph shows the fluorescence emission, in arbitrary units, of ThT bound to the amyloid formed in the presence of the peptides indicated in the *x* axis. The value shown correspond to the average ± standard deviation of three different experiments made in duplicated.

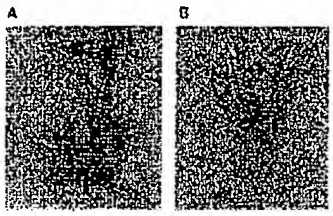

FIG. 3. **Electron micrographs of negative-stained preparations of fibrils assembled from SP40 and SP40A.** Aliquots of both peptides: SP40 (*A*) and SP40A (*B*), were adsorbed onto 300-mesh Formvar-coated grids and negative-stained with 2% uranyl acetate. The specimens were viewed for fibrils with a Phillips electron microscope. Magnification, × 66,000.

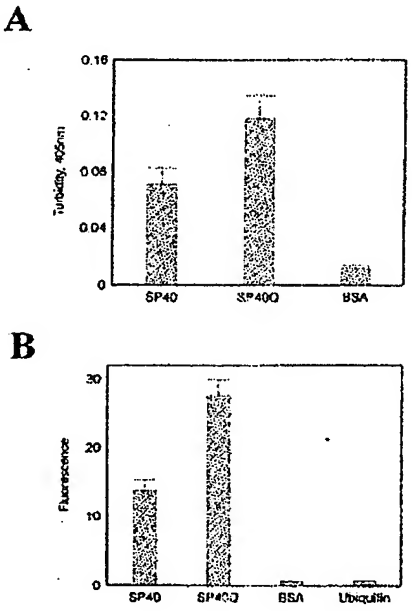

FIG. 4. **Aggregation and amyloid formation by SP40 and SP40Q.** This figure was performed under the same experimental conditions described in Fig. 2. In the turbidity measurement (*A*) the time of incubation was 24 h. In the fluorescence studies (*B*) the incubation time was 15 h. Both experiments were performed in a peptide concentration of 1 mg/ml. The mean ± standard deviation of three different experiments made in duplicated is shown.

Both SP40 (Fig. 3*A*) and SP40A (Fig. 3*B*) were able to form amyloid fibrils with the typical features described by these fibers (7, 16). Although the morphology of the amyloid fibers was identical, the amount of this structure obtained in the electron microscopic grids was higher in SP40 than in SP40A, which strengthened the results described above.

In order to additionally study the influence of the secondary structure of the N-terminal domain on the rate of amyloid formation, we analyzed the effect produced by the glutamine/glutamic acid substitution at residue 22 of Aβ. This substitution is found in hereditary cerebral hemorrhage with amyloidosis, Dutch type (22). Previous studies with synthetic peptides have shown accelerated fibril formation in a 28-residue peptide homologous to the Dutch variant Aβ (23). Our CD studies indicates that the Dutch mutation diminishes the level of α-helical conformation in comparison to the wild-type human peptide (Fig. 1*B*). In fact, the α-helical content of a synthetic peptide containing the sequence 1–40 of Aβ but bearing the Dutch mutation (SP40Q), in the presence of 20% TFE was only 5.9%, in comparison with the 16.6% present in SP40. This result is in agreement with previous studies showing a higher amount of β-sheet in the Dutch variant than the normal Aβ obtained by FT-IR and CD spectroscopy (24, 25). To evaluate the effect of this change in the secondary structure, we compared the ability to form amyloid between SP40 and a SP40Q. The turbidity measurements showed that SP40Q became aggregated at a higher level than SP40 (Fig. 4*A*) after 24 h of incubation. The amyloid quantification using the ThT method showed that SP40Q formed 100% more amyloid than SP40 (Fig. 4*B*) after 15 h of incubation. This result indicates that the 1–40 peptide of the Dutch variant Aβ has accelerated amyloid fibril formation, as was previously shown for shorter peptides consisting of residues 1–28 and 21–28 (23). No differences were detected in the morphology of the amyloid fibrils formed for SP40Q. in comparison with SP40 (data not shown), which is consistent with previous studies (23, 24).

DISCUSSION

In the present work we demonstrate that a single mutation of valine 18 to alanine produces a homologous Aβ peptide that is less able to form amyloid *in vitro*. This substitution does not significantly modify either the ionic or the hydrophobic properties of Aβ. However, this modification increases the α-helical content of Aβ as was observed through FT-IR and CD spectroscopy. Considering the position of the substitution and the analysis by secondary structure prediction, it is widely possible that the change in conformation occurs in the N-terminal domain of

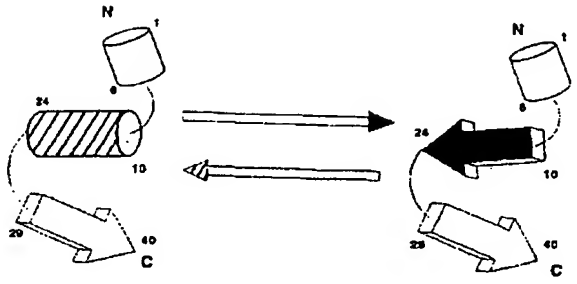

RISK FACTORS FOR FIBRILLOGENESIS

a) Environmental

- pH, concentration
- binding to pathological chaperones: (apoE or J, AP, GAG, etc.)
- chemical modifications

b) Genetic

- mutations of the βPP gene
- homozygosity (or hetero) for the E4 allele
- gene located on chromosome 14

FIG. 5. **Schematic representation of the conformational equilibrium between alternative structures for Aβ, indicating some possible regulators of the transition.** The structure shown at *left* should be the soluble form of Aβ, which is released by normal cells and is detected as a soluble entity in cerebrospinal fluid from normal and AD individuals (32, 33). On the other hand, the structure shown at *right* should be the form of Aβ able to form aggregates (34, 35), once the effective local concentration allows interactions between chains.

Aβ, which in SP40A would adopt mainly an α-helical structure. By contrast, in the Dutch variant of Aβ, the glutamine for glutamic acid substitution at residue 22 diminishes the propensity of the N-terminal region of Aβ to adopt the α-helical conformation concomitantly with an increase in amyloid formation. These findings suggest the existence of a correlation between the secondary structure of the N-terminal domain (amino acids 10–24) of Aβ and its ability to form amyloid fibrils.

In view of the foregoing results, we postulate that Aβ exists in an equilibrium between two alternative species in solution: one able to form amyloid, which presents a β-strand conformation in its N-terminal domain; and another one unable to form amyloid, which adopts an α-helical structure in this region (Fig. 5). In fact, our recent studies have shown that after long incubation times, the non-sedimentable peptide fractions contain a large amount of α-helical and random coil structure, completely different to the structure of the sedimentable fraction, which presents almost completely a β-sheet conformation. Recently, it has been proposed that in another type of amyloidosis the conversion of an α-helix into a β-strand is a feature of the transformation of the normal cellular prion proteins into the pathological scrapie prion proteins (26).

The existence of an equilibrium between alternatives conformations for Aβ is additionally supported by a recent study of the tridimensional structures of Aβ and its Dutch variant through NMR (27). Furthermore, the finding that the aggregated Aβ is in equilibrium with a non-sedimentable form of the peptide (7, 28) supports the idea that in solution there are two species of Aβ differing in their abilities to form amyloid. When the N-terminal segment of Aβ adopts a β-strand conformation, Aβ may exist as an anti-parallel β-sheet capable of interacting with other peptides forming a cross-β supersecondary structure. This structure has been proposed for the amyloid fibril, based on its x-ray diffraction pattern (29, 30).

It has been shown previously that Aβ analogs in which hydrophobic residues (phenylalanine 19 and 20) were substituted by non-hydrophobic amino acids exhibit a markedly increased solubility as determined by sedimentation assays (8). Accordingly, it was proposed that the formation of aggregates depends upon a hydrophobic effect that leads to intra- and intermolecular interactions between hydrophobic parts of Aβ. Although the effect obtained with SP40A could be explained by modifications in the hydrophobic properties induced by the substitution, this appears unlikely because the putative hydrophobicity changes in this case are small. Another study showing the effect of Aβ(1–28) with alanine substituted by lysine at position 16 has been reported previously (31). In that case, the modified peptide formed β-pleated sheet assemblies that were dissimilar to those formed by non-modified Aβ(1–28) and enhanced the packing of the sheets. However, in that work, the effect of the substitution in the aggregation kinetics was not studied.

Our data show that the N-terminal domain of Aβ may be important for modulation of peptide aggregation and amyloid fibril formation. This is an alternative view to the current model in which the determinant role for Aβ aggregation is placed on its C-terminal segment (6, 7, 13, 28).

Our hypothesis may explain how the same amino acid sequence can exist in a soluble (32, 33) and an insoluble form (34, 35). In fact, small perturbations in the conformational equilibrium could determine big changes in the ability of Aβ to form amyloid fibrils. These modifications of the equilibrium shown in Fig. 5 could, for example, be caused by local pH changes, alterations of environmental hydrophobicity, or binding to other proteins, which could act as pathological chaperones such as proteoglycans (36) and apolipoprotein E (37). The factors that eventually produce alterations in the conformational equilibrium of Aβ could be important risk factors in the development of AD, and could explain why not all persons shown the disease.

Finally, if the amyloid deposition is sensitive to the secondary structure adopted by the N-terminal domain of Aβ, as proposed in this work, compounds that promote the α-helical conformation in this region could prevent amyloid fibril formation. In fact, in the presence of 1,1,1,3,3,3-hexafluoro-2-propanol, an α-helix promoting solvent, Aβ is completely soluble up to a concentration of 40 mg/ml (28). Thus, the hypothesis proposed in this paper opens a potential new avenue to search for therapeutic agents that can promote α-helix formation in the N-terminal domain of Aβ and could stop or delay the advance of AD.

Acknowledgments—We are grateful to Dr. Jorge Garrido from the Department of Cellular and Molecular Biology of the Catholic University of Chile, for aid with the electron microscope. We also appreciate the collaboration of Dr. Octavio Monasterio and Patricio Rodriguez from the Department of Biology of the Faculty of Sciences, University of Chile, for help with the FT-IR studies. Finally, we thank Drs. Thomas Wisniewski, Jaime Alvarez, and Hugo L. Fernández for helpful comments on the manuscript.

REFERENCES

1. Inestrosa, N. C., and Soto, C. (1992) *Biol. Res.* 25, 63–72
2. Müller-Hill, B., and Beyreuther, K. (1989) *Annu. Rev. Biochem.* 58, 287–307
3. Chou, P., and Fasman, G. (1978) *Annu. Rev. Biochem.* 47, 251–276
4. Garnier, J., Osguthorpe, D. J., and Robson, B. (1978) *J. Mol. Biol.* 120, 97–120
5. Soto, C., Brañes, M. C., Alvarez, J., and Inestrosa, N. C. (1994) *J. Neurochem.* 63, 1191–1198
6. Halverson, K., Fraser, P., Kirschner, D., and Lansbury, Jr., T. (1990) *Biochemistry* 29, 2639–2644
7. Hilbich, C., Kisters-Woike, B., Reed, J., Masters, C. L., and Beyreuther, K. (1991) *J. Mol. Biol.* 218, 149–163
8. Barrow, C., and Zagorski, M. (1991) *Science* 253, 179–182
9. Zagorski, M., and Barrow, C. (1992) *Biochemistry* 31, 5621–5631
10. Barrow, C., Yasuda, A., Kenny, P., and Zagorski, M. (1992) *J. Mol. Biol.* 225, 1075–1093
11. Fraser, P. E., Nguyen, J. T., Surewicz, W. K., and Kirschner, D. A. (1991) *Biophys. J.* 60, 1190–1201

12. Greenfield, N., and Fasman, G. D. (1969) *Biochemistry* **8**, 4108–4116
13. Jarrett, J., Berger, E., and Lansbury, P., Jr. (1993) *Biochemistry* **32**, 4693–4697
14. Naiki, H., Higuchi, K., Nakakuki, K., and Takeda, T. (1991) *Lab. Invest.* **65**, 104–110
15. LeVine, H. (1993) *Protein Sci.* **2**, 404–410
16. Castaño, E. M., Ghiso, J., Prelli, F., Gorevic, P. D., Migheli, A., and Frangione, B. (1986) *Biochem. Biophys. Res. Commun.* **141**, 782–789
17. Tobias, D. J., and Brooks, C. L. (1991) *Biochemistry* **30**, 6069–6070
18. Horovitz, A., Matthews, J. M., and Fersht, A. R. (1992) *J. Mol. Biol.* **227**, 560–568
19. Blaber, M., Zhang, X., and Matthews, B. (1993) *Science* **260**, 1637–1640
20. Padmanabhan, S., Marqusee, S., Ridgeway, T., Laue, T. M., and Baldwin, R. L. (1990) *Nature* **344**, 268–270
21. Nelson, J. W., and Kallenbach, N. R. (1989) *Biochemistry* **28**, 5256–5261
22. Levy, E., Carman, M., Fernandez-Madrid, I., Power, M., Lieberburg, I., van Duinen, S., Gerard, T., Bots, A., Luyendijk, W., and Frangione, B. (1990) *Science* **248**, 1124–1128
23. Wisniewski, T., Ghiso, J., and Frangione, B. (1991) *Biochem. Biophys. Res. Commun.* **179**, 1247–1254
24. Fraser, P. E., Nguyen, J. T., Inouye, H., Surewicz, W. K., Selkoe, D. J., Podlisny, M. B., and Kirschner, D. A. (1992) *Biochemistry* **31**, 10716–10723
25. Fabian, H., Szendrei, G. I., Mantsch, H. H., and Otvos Jr., L. (1993) *Biochem. Biophys. Res. Commun.* **191**, 232–239
26. Pan, K. W., Baldwin, M., Nguyen, J., Gasset, M., Serban, A., Groth, D., Mehlhorn, I., Huang, Z. W., Fletterick, R. J., Cohen, F. E., Prusiner, S. B. (1993) *Proc. Natl. Acad. Sci. U. S. A.* **90**, 10962–10966
27. Sorimachi, K., and Craik, D. J. (1994) *Eur. J. Biochem.* **219**, 237–251
28. Burdick, D., Soreghan, B., Kwon, M., Kosmoski, J., Knauer, M., Henschen, A., Yates, J., and Glabe, C. (1992) *J. Biol. Chem.* **267**, 546–554
29. Kirschner, D. A., Abraham, C., and Selkoe, D. J. (1986) *Proc. Natl. Acad. Sci. U. S. A.* **83**, 503–507
30. Gorevic, P. D., Castaño, E. M., Sarma, R., and Frangione, B. (1987) *Biochem. Biophys. Res. Commun.* **147**, 854–862
31. Kirschner, D. A., Inouye, H., Duffy, L. K., Sinclair, A., Lind, M., and Selkoe, D. J. (1987) *Proc. Natl. Acad. Sci. U. S. A.* **84**, 6953–6957
32. Seubert, P., Vigo-Pelfrey, C., Esch, F., Lee, M., Dovey, H., Davis, D., Sinha, S., Schlossmacher, M., Whaley, J., Swindlehurst, C., McCormack, R., Wolfert, R., Selkoe, D., Lieberburg, I., and Schenk, D. (1992) *Nature* **359**, 325–327
33. Shoji, M., Golde, T., Ghiso, J., Cheung, T., Estus, S., Shaffer, L., Cai, X., McKay, D., Tinter, R., Frangione, B., and Younkin, S. (1992) *Science* **258**, 126–129
34. Glenner, G., and Wong, C. (1984) *Biochem. Biophys. Res. Commun.* **120**, 885–890
35. Masters, C., Simms, G., Weinman, N., Multhaup, G., McDonald, B., and Beyreuther, K. (1985) *Proc. Natl. Acad. Sci. U. S. A.* **82**, 4245–4249
36. Brandan E., and Inestrosa, N. C. (1993) *Gen. Pharmacol.* **24**, 1063–1068
37. Wisniewski, T., and Frangione, B. (1992) *Neurosci. Lett.* **135**, 235–238

EXHIBIT D

228

J. Mol. Biol. (1992) 225, 1075–1093

Solution Conformations and Aggregational Properties of Synthetic Amyloid β-Peptides of Alzheimer's Disease

Analysis of Circular Dichroism Spectra

Colin J. Barrow†, Akikazu Yasuda, Peter T. M. Kenny and Michael G. Zagorski‡

Suntory Institute for Bioorganic Research
Wakayamadai, Shimamoto-cho, Mishima-gun
Osaka 618, Japan

(Received 24 September 1991; accepted 12 February 1992)

The A4 or β-peptide (39 to 43 amino acid residues) is the principal proteinaceous component of amyloid deposits in Alzheimer's disease. Using circular dichroism (c.d.), we have studied the secondary structures and aggregational properties in solution of 4 synthetic amyloid β-peptides: β-(1–28), β-(1–39), β-(1–42) and β-(29–42). The natural components of cerebrovascular deposits and extracellular amyloid plaques are β-(1–39) and β-(1–42), while β-(1–28) and β-(29–42) are unnatural fragments.

The β-(1–28), β-(1–39) and β-(1–42) peptides adopt mixtures of β-sheet, α-helix and random coil structures, with the relative proportions of each secondary structure being strongly dependent upon the solution conditions. In aqueous solution, β-sheet structure is favored for the β-(1–39) and β-(1–42) peptides, while in aqueous solution containing trifluoroethanol (TFE) or hexafluoroisopropanol (HFIP), α-helical structure is favored for all 3 peptides. The α-helical structure unfolds with increasing temperature and is favored at pH 1 to 4 and pH 7 to 10; the β-sheet conformation is temperature insensitive and is favored at pH 4 to 7. Peptide concentration studies showed that the β-sheet conformation is oligomeric (intermolecular), whereas the α-helical conformation is monomeric (intramolecular). The rate of aggregation to the oligomeric β-sheet structure (α-helix → random coil → β-sheet) is also dependent upon the solution conditions such as the pH and peptide concentration; maximum β-sheet formation occurs at pH 5·4. These results suggest that β-peptide is not an intrinsically insoluble peptide. Thus, solution abnormalities, together with localized high peptide concentrations, which may occur in Alzheimer's disease, may contribute to the formation of amyloid plaques.

The hydrophobic β-(29–42) peptide adopts exclusively an intermolecular β-sheet conformation in aqueous solution despite changes in temperature or pH. Therefore, this segment may be the first region of the β-peptide to aggregate and may direct the folding of the complete β-peptide to produce the β-pleated sheet structure found in amyloid deposits. Differences between the solution conformations of the β-(1–39) and β-(1–42) peptides suggests that the last 3 C-terminal amino acids are crucial to amyloid deposition.

Keywords: β-peptide; Alzheimer's disease; circular dichroism

1. Introduction

Alzheimer's disease (AD§) is a major cause of ile dementia, and is characterized by pathologic n lesions composed of amyloid deposits (for reviews, see Glenner, 1988; Müller-Hill & Beyreuther, 1989; Selkoe, 1989; Ishiura, 1991). The

† Present address: Sterling Drug Inc., 9 Great Valley Parkway, Malvern, PA 19355, U.S.A.

‡ Author to whom correspondence should be addressed.

§ Abbreviations used: AD, Alzheimer's disease; APP, amyloid precursor protein; c.d., circular dichroism; PAM, phenylacetamidomethyl; TFA, trifluoroacetic acid; TFE, trifluoroethanol; n.m.r., nuclear magnetic resonance; FAB-MS, fast-atom bombardment mass spectrometry; HFIP, hexafluoro-2-propanol.

0022-2836/92/121075-19 $03.00/0

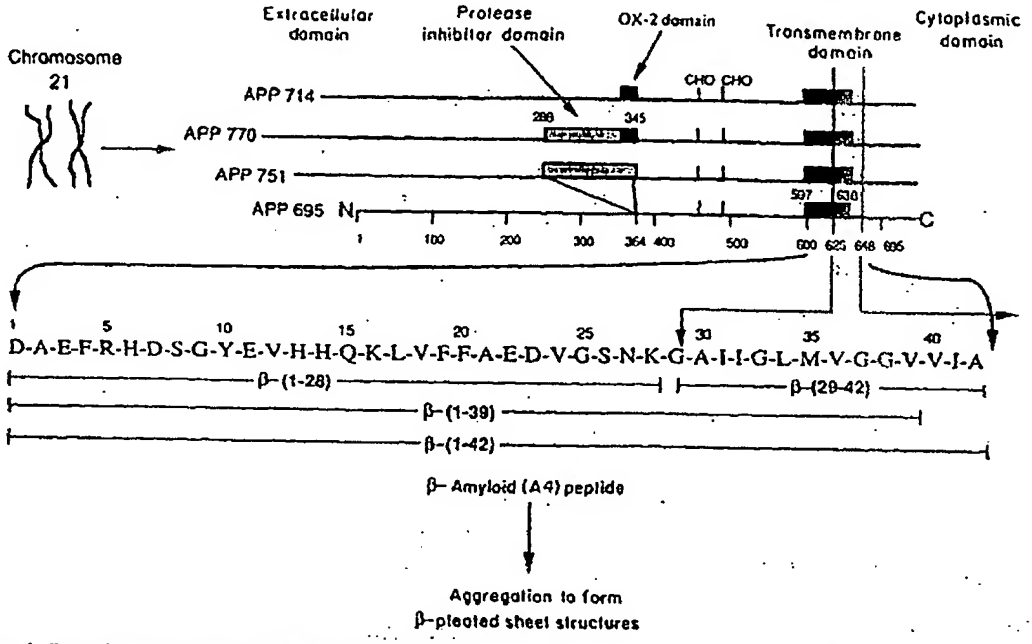

Figure 1. Overview of the biogenesis of β-peptide, as derived from proteolysis of APP. The amino acid sequences of the 4 peptides β-(1–28), β-(29–42), β-(1–39), and β-(1–42) investigated in this study are also shown.

major protein constituent of amyloid deposits is the A4 (Masters *et al.*, 1985) or β-peptide (Glenner & Wong, 1984*a*), which is a small polypeptide consisting of 39 to 43 amino acid residues (see Fig. 1; the peptides composed of 39 and 42 residues are abbreviated as β-(1–39) and β-(1–42)). Extracellular deposits consist of amyloid plaques and cerebrovascular amyloid, whereas intracellular deposits consist of neurofibrillary tangles. Similar amyloid plaques, also composed of β-peptide, occur in the brains of individuals afflicted with Down's syndrome (Glenner & Wong, 1984*b*), and in smaller amounts in the brains of normal older humans (Coria *et al.*, 1988) and other mammals (Selkoe *et al.*, 1987).

β-Peptide is derived from the *in vivo* proteolysis of a larger amyloid precursor protein (APP) (Kang *et al.*, 1987). The gene for APP has been sequenced to chromosome 21, and it can be copied into five mRNA forms, which produce APPs of different primary structure: APP563, APP695, APP714, APP751, and APP770 (the numbers 563, 695, 714, 751 and 770 refer to the number of amino acid residues, see Fig. 1). APP563, APP751 and APP770 contain an insert encoding a Kunitz type protease inhibitor domain, while APP714 and APP770 contain an OX-2-related domain (Kitaguchi *et al.*, 1988). APP563 is devoid of the transmembrane domain containing the β-peptide region (Weidemann *et al.*, 1989; Kitaguchi *et al.*, 1990; Ottersdorf *et al.*, 1990), and therefore is not amyloidogenic. Although in humans amyloid deposits are primarily found in brain tissue, the origin of APP is more diverse. For example, APP is found in brain and cerebrospinal fluid (Weidemann *et al.*, 1989), kidney, spleen, heart, adrenal tissues (Selkoe *et al.*, 1988), and platelets (Bush *et al.*, 1990).

Most of the recent research into AD has focused upon the relationship of different APP forms to AD, and upon the pathways in which APP is proteolytically processed (Palmert *et al.*, 1989; Johnson *et al.*, 1990; Sisodia *et al.*, 1990). Unfortunately, there still exists no clear-cut correlation between the levels of different APP forms to the amounts and types of amyloid deposits, and it is also unclear how an abnormal cleavage of APP could be responsible for β-peptide deposition. Less research effort has been directed toward an understanding of the dynamics of β-peptide in solution (Hollósi *et al.*, 1989; Hilbich *et al.*, 1991), since it is thought that β-peptide is a highly insoluble protein, and after cleavage from APP, spontaneously self-assembles into a β-pleated twisted fibril structure, the probable structure in plaques (Kirschner *et al.*, 1986). However, alternative mechanisms involving localized changes in pH, temperature, glycosylation of β-peptide (Behrouz *et al.*, 1989), or accumulation of aluminum silicates (Candy *et al.*, 1986), may be responsible for the precipitation of β-peptide. In the latter case β-peptide may be envisioned as a normal proteolytic product that precipitates due to solution abnormalities present in Alzheimer brain.

To provide a basis for understanding the relationships between the accumulation of amyloid fibrils in AD and the mechanisms involved in precipitation of β-peptide, we are currently studying the structure and dynamics of β-peptide in solution (for a pre-

liminary report, see Barrow & Zagorski, 1991). We report here the secondary structures of four synthetic β-peptides, β-(1–28), β-(29–42), β-(1–39) and β-(1–42), obtained in solution from analysis of circular dichroism (c.d.) spectra (see Fig. 1 for the amino acid sequences of these peptides). In patients with AD, β-(1–39) is a principal component of cerebrovascular deposits (Prelli *et al.*, 1988), whereas β-(1–42) is the principal component of amyloid plaques. The unnatural β-(1–28) and β-(29–42) peptides, which are composed of amino acid residues 1 to 28 and 29 to 42 of β-(1–42), occupy the extracellular and transmembrane domains within APP.

Our work demonstrates that β-peptide adopts mixtures of β-sheet, α-helix and random coil conformations in solution with relative ratios being strongly influenced by the solution conditions. Our results also suggest that the hydrophobic residues located at the C terminus of the parent β-(1–42) peptide may be involved in the initial stages of folding to produce the β-pleated sheet structure found in amyloid plaques. For the amino acid residues located at the N terminus, however, the rate of β-sheet formation is strongly dependent on factors such as the hydrophobicity and pH of the surrounding environment.

2. Materials and Methods

(a) *Syntheses and purification of β-peptides*

All 4 peptides, β-(1–28), β-(29–42), β-(1–39) and β-(1–42), were synthesized on solid phase in an automated fashion using a model 430A peptide synthesizer (Applied Biosystems Japan, Inc.) with standard computer software, using the conventional t-Boc strategy and phenylacetamidomethyl (PAM) resin. The amino acid cartridges and the reagents for peptide syntheses were purchased from Applied Biosystems. Side-chain protecting groups were *O*-benzyl- for Asp, Glu and Ser; 2-chlorocarbobenzoxy- for Lys; bromo-carbobenzoxy for Tyr; tosyl- for Arg; and dinitrophenyl for His. The peptides were cleft from the resin by removal of the dinitrophenyl protecting groups with thiophenol, then removal of the t-Boc protecting groups with trifluoroacetic acid (TFA) in dichloromethane, followed by treatment with anhydrous hydrogen fluoride (plus 10% *m*-cresol) for 1 h at 0°C. The peptides were extracted from the resin with TFA, then precipitated and washed repeatedly with diethyl ether. The β-(29–42) and β-(1–42) peptides were triturated and washed with water to improve solubility. Final purification was done on reverse-phase h.p.l.c. using mixtures of acetonitrile, trifluoroethanol (TFE), water and TFA, on C4 (Vydac) and 5C4-300 (Cosmosil) preparative columns obtained from The Separation Group (Hesperia, CA, U.S.A.).

(b) *Characterization of peptides*

The purified and deprotected peptides were analyzed by amino acid analysis (AAA), fast-atom bombardment mass spectrometry (FAB-MS), and proton nuclear magnetic resonance spectroscopy (^{1}H n.m.r.). The peptides were hydrolyzed at 110°C for 24 h in 6 M-HCl (containing 0·2% phenol) prior to the AAA, which was done using standard *o*-phthalaldehyde methods.

All ^{1}H n.m.r. measurements were made at 500 MHz on a General Electric GN-500 spectrometer. Chemical shifts are referenced to external sodium 3-(trimethylsilyl) propionate- 2,2,3,3-d_4. To avoid possible side-reactions with solvents (for an example, see Klunk & Pettegraw, 1990), all n.m.r. spectra were recorded immediately after peptide dissolution. For all peptides, no extraneous peaks indicative of minor impurities or truncated peptides were present. Comparison of the integral heights in the aromatic, αH, and CH_3 regions, showed that the peptides were at least 95% pure.

FAB-MS measurements were carried out on a JEOL HX110A/HX110A tandem mass spectrometer. The accelerating voltage was 10 kV. Ions were produced with xenon using a JEOL FAB gun at 6 kV. All spectra were measured in the positive-ion mode and recorded on a JEOL DA-5000 data system. Before addition of the matrix, the peptides were dissolved in dimethyl sulfoxide, formic acid, or trifluoroacetic acid. Either glycerol, or a mixture of glycerol and 3-nitrobenzyl alcohol, were used as a matrix. For tandem mass spectrometric studies (MS/MS), the $M+H^+$ ion was selected by the first mass spectrometer. Subsequently, this ion was collided with helium in a collision cell (located in the third field-free region and floated at 3 kV), then a linked scan was acquired at a constant ratio of magnetic to electric field strengths using the second mass spectrometer. Such MS/MS analysis allowed us to substantiate the identities of the peptides by 2 methods: (1) comparison of the expected and actual molecular weights (listed below for each peptide), and (2) confirmation of the peptide sequences. For the β-(1–28) and β-(29–42) peptides the monoisotopic molecular weights are shown, whereas for the larger β-(1–39) and β-(1–42) peptides the average molecular weights are shown. All peptides had excellent agreement between the predicted and determined amino acid content. Shown below are the FAB-MS and the AAA data (both predicted and determined) for the four peptides:

β-(1–28). FAB-MS (MH^+) *m/z* 3261·79; MW, 3260·53. AAA: Asx 4·0 (4), Ser 1·8 (2), Glx 4·2 (4), Gly 2·2 (2), Ala 2·0 (2), Val 2·6 (3), Leu 1·2 (1), Tyr 1·1 (1), Phe 3·0 (3), His 3·0 (3), Lys 2·1 (2), Arg 1·0 (1).

β-(29–42). FAB-MS (MH^+) *m/z* 1269·76; MW, 1268·75. AAA: Gly 4·1 (4), Ala 2·0 (2), Val 2·2 (3), Met 0·9 (1), Ile 2·2 (3), Leu 1·2 (1).

β-(1–39). FAB-MS (MH^+) *m/z* 4235.37; MW, 4234·76 (this peptide contains 4 carbons labeled with 99·8% ^{13}C). AAA: Asx 4·1 (4), Ser 2·4 (2), Glx 4·2 (4), Gly 6·4 (6), Ala 2·8 (3), Val 4·9 (5), Met 0·9 (1), Ile 1·8 (2), Leu 2·1 (2), Tyr 1·0 (1), Phe 3·2 (3), His 2·8 (3), Lys 2·2 (2), Arg 1·2 (1).

β-(1–42). FAB-MS (MH^+) *m/z* 4514·85; MW, 4514·10. AAA: Asx 4·2 (4), Ser 2·7 (2), Glx 4·4 (4), Gly 8·6 (6), Ala 3·6 (4), Val 4·9 (6), Met 1·1 (1), Ile 2·2 (3), Leu 2·4 (2), Tyr 1·2 (1), Phe 3·1 (3), His 2·9 (3), Lys 2·4 (2), Arg 1·4 (1).

(c) *Size exclusion chromatography*

The extent of aggregation of the β-(1–28), β-(1–39) and β-(1–42) peptides at pH 7·4 and 3·5 were determined by size exclusion chromatography. At pH 7·4 and 3·5, an ammonium acetate buffer (50 μM) and a solution of aqueous acetic acid (0·01 MV) were used, respectively. A column (1 cm × 50 cm) was packed with Sephadex G50-SF. The eluant was kept at a constant flow rate of 10 ml/h using a peristaltic pump (Iwaki, Inc., model PST-103), and was monitored by measuring the absorbance at 220 nm. The peptides or protein standards (1 to 2 mg) were applied to the column in 0·5 ml of buffer.

(d) *Circular dichroism measurements*

The trifluoroethanol (TFE) and hexafluoro-2-propanol (HFIP) used for sample preparation were of the highest grade from commercial sources. Water was both deionized and distilled to remove inorganic and organic impurities. All spectra were obtained with a Jasco spectropolarimeter, model J-600A, equipped with a data processor, model DP-501 (Jasco Inc., Tokyo, Japan). The temperature was controlled with a refrigerated circulating bath, and temperature readings were taken with a thermometer (±0·1 deg.C) at the entrance port to the jacket which surrounded the quartz cell. The synthetic β-(1–28) and β-(1–39) peptides were soluble in aqueous solution. However, the β-(1–42) and β-(29–42) peptides are less soluble in aqueous solution. To overcome these solubility problems, stock solutions of the peptides were prepared in HFIP. Portions from these solutions were removed and diluted a 1000-fold in the buffered water solution used for c.d. analysis. For solutions containing TFE or HFIP in buffered water, the amount of HFIP or TFE is reported as percent by volume. With the exception of spectra shown in Fig. 8, spectra were recorded 20 min after the peptides were dissolved in the aqueous buffer solutions. Peptide concentrations in the stock solutions were determined by amino acid analysis. All solutions contained 5 μM-potassium phosphate as buffer, and the pH was adjusted to the desired value with a pH meter (Horiba, Inc., model F-12). Quartz cells of either 0·05-, 0·1- or 1·0-cm path lengths were used, depending upon whether a concentrated or a dilute peptide solution was being measured. Spectra were recorded at 1-nm intervals over the wavelength range 190 to 260 nm.

(e) *Methods of circular dichroism analysis*

Results are expressed in terms of mean residue ellipticity ($[\theta]\lambda$) in units of deg·cm^2/decimol (dmol), and were determined according to the following equation: $[\theta]\lambda = (\theta\lambda)\ (MRW)/10lc$, where θ corresponds to the measured ellipticity angle at wavelength λ (mdeg), MRW is the mean residue weight, l is the optical path length (cm), and c is the protein concentration (g/ml). All spectra were obtained by subtracting buffer base-line spectra and no filtering or other smoothing technique (Savitzky & Golay, 1964) was used to reduce the noise levels.

The percent α-helical content was determined using both the 208 nm (Greenfield & Fasman, 1969) and the 220 nm (Morrisett *et al.*, 1973) absorptions according to the following equations: % α-helix = $([\theta]_{208} - 4000/-33{,}000 - 4000) \times 100$ and = $([\theta]_{222} - 3000/-36{,}000 - 3000] \times 100$. The method based on the 220 nm absorption assumes no β-sheet content, thus the 208 nm absorption was better suited for estimations of the α-helical content in the presence of β-sheet (see Table 1 for a summary of the calculations). The curves shown in Figs 2(c) (d), 3(c), (d), 6 and 7 were generated by manual curve fitting.

Estimates of β-sheet and random coil structures were obtained by a least-squares curve-fitting procedure (Chang *et al.*, 1978) using reference spectra of poly-L-lysine (Greenfield & Fasman, 1969). This latter procedure involved using a program supplied with the Jasco spectropolarimeter (Secondary Structure Estimation or SSE-98, Jasco, Inc.). In using this program, 2 operations were performed: (1) a constrained standard fitting mode (where the fraction of each secondary structure is positive and the sum of the fractions equals unity), and (2) a non-constrained fitting (where no constraint on the sum of the fractions or on the negative values is imposed). Generally, the results of the two fittings agreed to within ±10%, illustrating that satisfactory calculated spectra were obtained by this method (Yang *et al.*, 1986). This program also provided percentages of α-helix and β-turn. Typically, the amounts of α-helix determined with the SSE-98 program agreed to within ±10% with those obtained from the direct calculation as described above. However, since the reference spectra for poly-L-lysine contain essentially no β-turns, the percentages of β-turn determined from the program were always approximately zero, so these were not included for the present study of the amyloid β-peptides. Furthermore, analysis for β-turns in the c.d. spectra of small peptides often are unreliable (Woody, 1974). The SSE-98 program also provided a normalized standard deviation (NRMSD), which is a goodness-of-fit parameter (Brahms & Brahms, 1980). For the majority of calculations, NRMSD values were in the range of 0·1 to 0·2, indicating that the calculated structures were indeed consistent with actual structure.

3. Results

(a) *Selection of β-peptide fragments*

The sequences of the four peptides, β-(1–28), β-(29–42), β-(1–39) and β-(1–42), investigated in this study are shown in Figure 1. The β-(1–42) and β-(1–39) peptides were studied because they are natural components of amyloid deposits. We also decided to study the smaller β-peptide segments, β-(1–28) and β-(29–42), since they represent distinct regions of β-peptide. β-(29–42) contains only hydrophobic amino acids, while β-(1–28) contains mostly hydrophilic amino acids. Most significantly, the β-(1–28) peptide forms amyloid fibrils *in vitro* (Kirschner *et al.*, 1987; Gorevic *et al.*, 1987), whereas a peptide composed of residues 34 to 42 is known to aggregate and form thick twisted fibrils (Halverson *et al.*, 1990). We hoped to elucidate the relative contributions of each distinct peptide region to the aggregational properties of β-peptide.

(b) *Solvent composition*

We first investigated the influence of the structure forming solvents, TFE and HFIP, on the secondary structures of the amyloid β-peptides. c.d. spectra for the β-(1–42) and β-(1–39) peptides recorded at 22 °C, pH 7·3, and in buffered aqueous solution containing different amounts of TFE are shown in Figure 2(a) and (b). The percentages of secondary structures calculated for each c.d. trace are listed in Table 1, and are depicted graphically in Figure 2(c) and (d). In water without TFE, the β-(1–42) peptide adopts largely a β-sheet structure, whereas the β-(1–39) peptide has substantially less β-sheet structure (Table 1). Little or no helical structure is observed for the β-(1–39) and β-(1–42) peptides in water at pH 7·3.

For aqueous solutions containing TFE (Fig. 2(a) and (b)) there is a decrease in β-sheet content with an accompanying increase in α-helical content as the amount of TFE is increased, with maximum amount of α-helical structure observed for β-(1–39) and β-(1–42) at 90% TFE (Fig. 2(c)). For β-(1–39),

Table 1

Estimates of secondary structure in amyloid β-peptides from analysis of c.d. spectra

Peptide (μM)	Solvent	Temperature (°C)	pH	$[\theta]_{208}$ (deg·cm²/dmol)	$[\theta]_{222}$	α-Helix (%$[\theta]_{208}$)	(%$[\theta]_{222}$)	β-Sheet (%)	Random coil (%)
β-(1-28):									
A. *Solvent composition study*									
3·5	Water	22	2·8	−4300	−933	1	7	0	85
	10% TFE			−5800	−1600	6	12	0	65
	20% TFE			−13000	−11300	31	37	0	35
	30% TFE			−24500	−21650	70	63	0	20
	40% TFE			−20600	−18500	57	55	0	25
	60% TFE			−20600	−18550	57	58	0	25
B. *pH study*									
6·4	60% TFE	22	1·2	−29800	−25200	89	70	0	18
			3·2	−23800	−18900	68	56	4	17
			4·3	−13520	−16380	34	42	40	20
			4·7	−12700	−12700	30	40	44	40
			5·4	−12200	−10300	28	32	60	15
			6·2	−14300	−11900	39	37	54	15
			6·7	−15080	−12140	41	38	40	15
			7·0	−16900	−13300	44	42	5	39
			8·0	−20000	−14550	55	45	0	28
			10·2	−23800	−18900	60	56	5	40
C. *Peptide concentration study*									
666·0	60% TFE	22	2·8	−21100	−17600	58	53	0	25
333·0				−17822	−17810	49	53	0	25
167·0				−17802	−17372	49	52	0	25
83·0				−19052	−17903	52	53	0	25
17·0				−19900	−18048	54	55	0	25
8·3				−16880	−15988	46	47	0	30
1·7				−20895	−19010	57	56	0	25
666·0			7·4	−17100	−13000	46	41	0	40
333·0				−16957	−13018	46	41	0	40
167·0				−16339	−12992	44	41	0	40
83·0				−16587	−12054	45	40	0	40
17·0				−17401	−13020	47	41	0	40
8·3				−13353	−10446	36	33	0	45
1·7				−15032	−10809	41	34	0	45
666·0			5·4	−12000	−10800	32	42	48	16
333·0				−12266	−10419	33	40	40	20
167·0				−12731	−10929	34	35	38	30
83·0				−14320	−10902	38	35	30	32
17·0				−17216	−11313	46	36	32	30
8·3				−11138	−8579	30	27	30	43
1·7				−9421	−4457	26	14	27	47
D. *Temperature study*									
4·3	60% TFE	−2	2·8	−26500	−20300	84	75	0	20
		3		−26800	−24200	78	70	0	25
		13		−22500	−20000	64	59	0	35
		22		−20700	−17300	57	52	0	40
		35		−17200	−12500	45	40	0	50
		50		−14300	−9800	35	33	0	60
		−3	7·4	−24000	−19000	68	55	0	35
		5		−20700	−16200	57	48	0	45
		15		−19200	−14300	52	44	5	50
		22		−18800	−12700	51	40	5	50
		50		−13000	−8000	30	28	10	70
β-(1-39):									
A. *Solvent composition study*									
5·2	Water	22	7·3	−1000	−3300	0	16	57	43
	10% TFE			−3800	−5400	0	22	59	39
	15% TFE			−10000	−7800	21	28	8	46
	20% TFE			−14700	−10800	37	35	0	21
	30% TFE			−16700	−12700	43	40	0	18
	40% TFE			−17800	−13800	48	43	0	31
	60% TFE			−18600	−14300	50	44	0	30
	80% TFE			−19800	−15200	55	47	0	30
5·2	Water	22	2·8	−1000	−3000	0	15	25	72
	10% HFIP			−19600	−16600	54	50	5	35
	20% HFIP			−22000	−18500	62	55	0	30

Table 1 *continued*

Peptide (μM)	Solvent	Temperature (°C)	pH	$[\theta]_{208}$ (deg·cm²/dmol)	$[\theta]_{222}$	α-Helix (%$[\theta]_{208}$)	(%$[\theta]_{222}$)	β-Sheet (%)	Random coil (%)
	30% HFIP			−23900	−20000	69	54	0	30
	40% HFIP			−24600	−20400	71	60	0	30
	60% HFIP			−22900	−18900	65	56	0	30
B. *pH study*									
5·2	25% TFE	22	1·3	−21200	−17700	59	53	0	24
			3·0	−17700	−14400	47	45	5	15
			5·5	−8400	−7900	12	28	40	30
			7·6	−16000	−11800	41	38	15	47
			8·3	−16100	−11800	42	38	7	25
			9·6	−17700	−13400	47	42	5	38
β-(1-42):									
A. *Solvent composition study*									
9	Water	22	2·8	−900	−4000	0	18	86	14
	10% TFE			−1400	−5700	0	20	88	12
	15% TFE			−2300	−6200	0	24	95	5
	20% TFE			−9800	−9900	20	33	45	31
	30% TFE			−16800	−13500	44	42	5	26
	40% TFE			−15400	−12400	39	40	2	29
	60% TFE			−14000	−12100	35	39	13	30
	90% TFE			−15600	−12400	40	40	0	21
10	Water	22	7·3	−800	−3000	0	16	79	21
	10% TFE			−600	−6200	0	21	83	17
	15% TFE			−4000	−7200	0	26	76	25
	20% TFE			−4800	−7000	3	26	63	33
	30% TFE			−11600	−10400	26	34	24	37
	40% TFE			−12000	−10200	28	34	12	36
	60% TFE			−14900	−11900	38	38	3	35
	90% TFE			−16000	−12400	41	39	0	22
14	Water	22	2·8	−1000	−3900	0	17	82	18
	10% HFIP			−11100	−10400	24	34	55	35
	20% HFIP			−15400	−12800	41	40	22	33
	30% HFIP			−16700	−13300	44	42	14	33
	40% HFIP			−16900	−13600	44	42	10	32
	60% HFIP			−16900	−13300	44	42	5	32
B. *pH study*									
12	Water	22	1·4	−1000		0	0	78	22
			2·9	−1100		0	0	80	20
			5·0	+2000		0	0	95	5
			7·3	+2000		0	0	90	10
			10·0	−800		0	0	73	27
			12·0	−1700		0	0	73	27
15	25% TFE	22	1·3	−12100	−10900	28	38	40	30
			3·0	−11300	−10500	25	37	50	30
			5·5	−500	−5300	0	21	80	10
			7·6	−10800	−11600	23	38	50	25
			8·3	−12000	−10400	28	37	40	35
			9·6	−13900	−11100	34	38	40	30
β-(29-42):†									
A. *Solvent composition* study									
10	Water	22	7·3	+400		0		100	0
	20% TFE			+4000		2		77	19
	40% TFE			−7200		14		72	22
	60% TFE			−8300		15		61	28
	80% TFE			−7700		13		40	36
	90% TFE			−8000		14		38	45
	100% TFE			−9300		18		25	52
22	Water	22	7·3	+100		0		100	0
	10% HFIP			−5800		0		65	30
	20% HFIP			−9300		15		63	25
	30% HFIP			−10300		20		60	30
	40% HFIP			−10300		20		45	42
	50% HFIP			−10000		20		23	53
	60% HFIP			−9900		20		26	54
	70% HFIP			−9100		17		28	54
	80% HFIP			−7900		12		29	54
	90% HFIP			−7200		10		34	54
	100% HFIP			−7300		10		30	55

Table 1 *continued*

Peptide (μM)	Solvent	Temperature (°C)	pH	$[\theta]_{208}$ (deg·cm²/dmol)	$[\theta]_{222}$	α-Helix (%$[\theta]_{208}$)	(%$[\theta]_{222}$)	β-Sheet (%)	Random coil (%)
B. Peptide concentration study									
590	60% HFIP	22	7·3	−10000		20		57	33
210				−11400		25		48	44
80				−13000		30		32	56
18				−11200		25		24	03

The percentages of α-helix were determined from the measured ellipticities at 208 and 222 nm, whereas the percentages of β-sheet and random coil were determined with a computer program (see Materials and Methods). Due to the different methods of calculation, the summation of the percentages for secondary structures may not equal 100%. We estimate that the results are accurate ±10%. When significant quantities of β-structure are present, the $[\theta]_{208}$ is better suited for estimating the amount of α-helix. c.d. measurements were performed no later than 20 min after sample peptide dissolution. All solutions contained 5 mM aqueous buffer and the amounts of TFE or HFIP are given as percent by volume.

† Since spectra for β-(29–42) did not change with variations in pH or temperature, all measurements shown for β-(29–42) were done at 22°C and pH 7·3.

in solutions containing 20 to 90% TFE, there is probably a mixture of only two conformations, α-helix and random coil. This conclusion is supported by the presence of an isodichroic point, which is a point where the $[\theta]$ intensities are equal. On the other hand, for β-(1–42), an isodichroic point is only apparent in solutions containing greater than 40% TFE. The drop in β-sheet content is more abrupt for β-(1–39) than for β-(1–42). The transition occurs within the 10 and 20% TFE range for β-(1–39) (Fig. 2(d)), where the β-sheet content is 59 and 8%, respectively. For β-(1–42) a more gradual loss in the β-sheet content occurs as the TFE content is increased. These results suggest that the

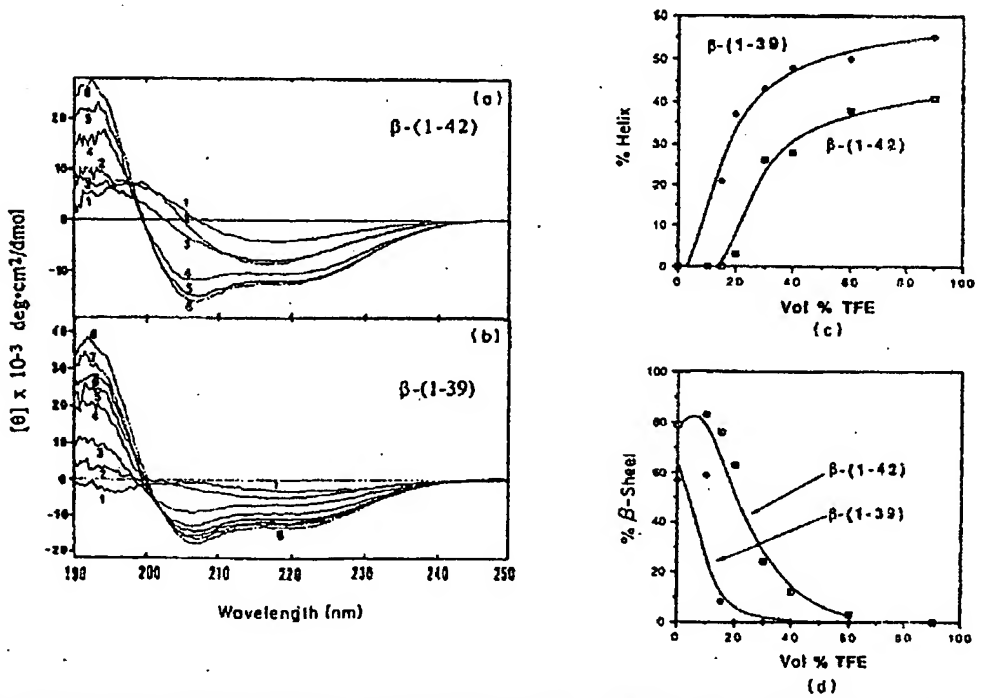

Figure 2. Solvent composition studies showing the effects of TFE on the secondary structures of the β-(1–42) and the β-(1–39) peptides. The c.d. spectra ((a) and (b)) and data (shown graphically in panels (c) and (d)) were obtained at pH 7·3, 22°C, and in buffered water solution containing different amounts of TFE (given as percent (%) by vol.) relative to water. Peptide concentrations were 5·2 and 10 μM for β-(1–39) and β-(1–42), respectively. In (a) (upper) spectra are shown for β-(1–42), and in (b) (lower) spectra are shown for β-(1–39). The amounts of α-helix, β-sheet, and random coil structures derived from the spectra are listed in Table 1 under Solvent composition study. The numbers listed on the spectra correspond to different amounts of TFE (c.d. trace, % TFE): (a) 1, 0%; 2, 15%; 3, 20%; 4, 30%; 5, 60%; 6, 90%; (b), 1, 0%; 2, 10%; 3, 15%; 4, 20%; 5, 30%; 6, 40%; 7, 60%; 8, 90%. The graphs in (c) and (d) show the effects of TFE on the percentages of α-helix and β-sheet (spectra for β-(1–42) that contained 10 and 40% TFE were omitted from (a), but are present in Table 1 and the graphs in panels (c) and (d)).

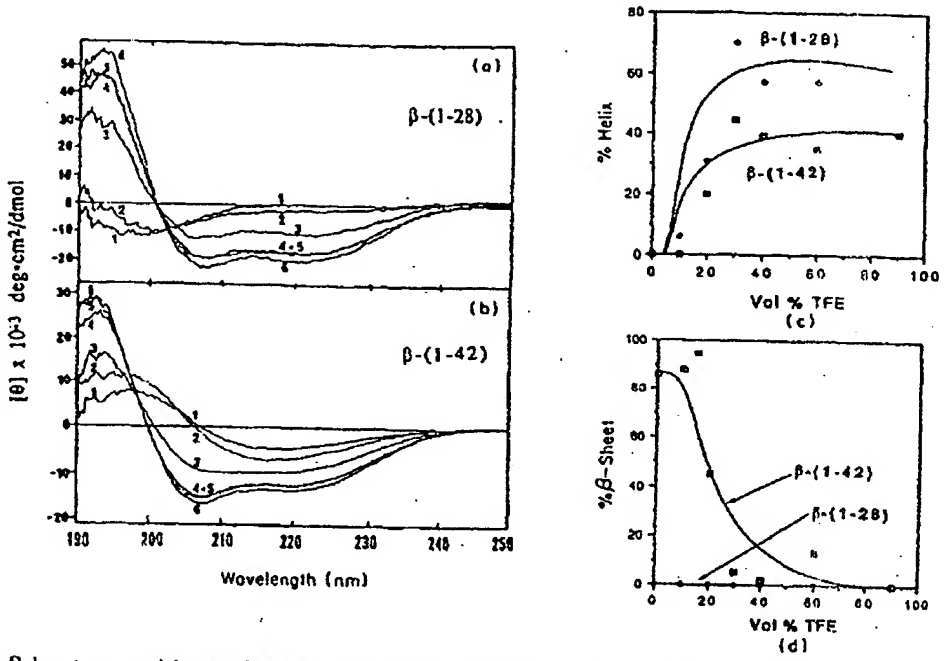

Figure 3. Solvent composition studies showing the effects of TFE on the secondary structures of the β-(1–28) and β-(1–42) peptides. The c.d. spectra ((a) and (b)) data (shown graphically in panels (c) and (d)) were obtained at pH 2·8, 22°C, and in buffered water solution containing different amounts of TFE (given as percent (%) by vol.) relative to water. Peptide concentrations were 3·5 and 9·0 μM for β-(1–28) and β-(1–42), respectively. In (a) (upper) spectra are shown for β-(1–28), and in (b) (lower) spectra are shown for β-(1–42). The amounts of α-helix, β-sheet, and random coil structures derived from the spectra are listed in Table 1 under Solvent composition study. The numbers listed on the spectra correspond to different amounts of TFE (c.d. trace, % TFE): (a) 1, 0%; 2, 10%; 3, 20%; 4, 30%; 5, 40%; 6, 60%; (b), 1, 0%; 2, 15%; 3, 20%; 4, 40%; 5, 90%; 6, 30%. The graphs in (c) and (d) show the effects of TFE on the percentages of α-helix and β-sheet (spectra for β-(1–42) that contained 10 and 60% TFE were omitted from (b)).

β-sheet structure for β-(1–42) is more stable in solution than the β-sheet structure for β-(1–39). Similar trends were observed using HFIP, with the exception that HFIP is a better α-helix forming solvent than is TFE (Table 1). Approximately 60% and 15% HFIP are required to significantly reduce the amounts of β-structure for β-(1–42) and β-(1–39), respectively, again showing that the β-sheet structure is more stable in β-(1–42) than in β-(1–39).

c.d. spectra for the β-(1–28) and β-(1–42) peptides obtained in water and water plus TFE at pH 2·8 are shown in Figure 3(a) and (b), respectively. These peptides differ considerably in their secondary structures in water at pH 2·8; the β-(1–42) peptide adopts primarily a β-sheet structure (86%), and the β-(1–28) peptide has virtually no β-sheet structure and is mostly random coil structure (85%). For β-(1–28), in 10% TFE solution the random coil structure is still predominant but, as shown in Figure 3(c) and listed in Table 1, approximately 31 to 37% helical structure is observed in 20% TFE solution, and the transition from random coil to helix reaches a maximum at 30% TFE with 63 to 70% helical structure being present. The helical content drops slightly with increased concentration of TFE. A similar effect was seen for the β-(1–42) peptide at pH 2·8 (Fig. 3(c)). No β-structure was observed for the β-(1–28) peptide in aqueous TFE at pH 2·8, and an isodichroic point was present at 202 nm for the 20, 30, 40 and 60% TFE solutions, indicating that only two conformations (random coil and α-helical) are present. With the addition of TFE to the aqueous solutions containing β-(1–42), there are increases in helical structure (Fig. 3(c)) and decreases in β-sheet structure (Fig. 3(d)).

Shown in Figure 4 are c.d. spectra for the β-(29–42) peptide, the smallest amyloid peptide investigated in the present work. As expected, since the peptide is completely hydrophobic, no changes occurred when the pH or temperature were varied. In water, the β-(29–42) peptide is 100% β-sheet as shown by the broad negative band at 217 nm and the positive band at 194 nm. When incremental portions of TFE (Fig. 4(a), upper) or HFIP (Fig. 4(b), lower) are added to the aqueous solutions, there is a progressive shift from β-sheet structure to random coil. This effect is more pronounced with HFIP. The absence of any notable absorptions at 208 or 222 nm suggests that little or no α-helical structure exists. However, there is a small increase in the 208 nm absorption (first maximum for α-helix) with increasing amounts of HFIP, but the

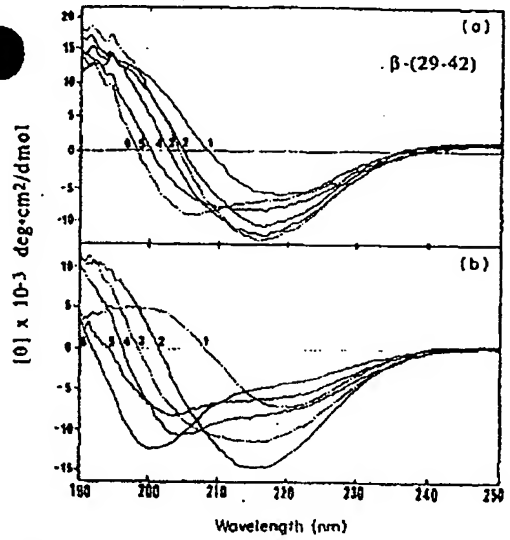

Figure 4. c.d. spectra of the β-(29–42) peptide in aqueous solution with various concentrations (percent by volume) of TFE (a) and HFIP panel ((b) lower). The proportions of secondary structures derived from each spectrum are summarized in Table I. Data were obtained at 22°C, pH 7·3, and peptide concentrations of 10 μM ((a); upper) and 22 μM ((b), lower). The amounts of TFE and HFIP used for each spectrum are as follows (spectrum number, % by volume of TFE or HFIP): ((a), upper) 1, 0%; 2, 20%; 3, 40%; 4, 60%; 5, 90%; 6, 100%; ((b), lower) 1, 0%; 2, 30%; 3, 40%; 4, 50%; 5, 90%; 6, 100%.

lack of any absorption at 222 nm (second maximum for α-helix) indicates that no α-helical structure is present. Instead, the absorption at 208 nm could be the result of a slight shift of the 217 nm absorption (maximum for β-sheet), since this peak is sensitive to changes in solvent (Li & Spector, 1969; Quadrifoglio & Urry, 1968).

(c) *Effects of pH*

The importance of charge effects or side-chain ionizations on the secondary structures were evaluated by measuring c.d. spectra as a function of pH. Shown in Figure 5 are c.d. spectra of β-(1–28), β-(1–39) and β-(1–42) recorded in aqueous-TFE solutions at different pH values, and the amounts of α-helix and β-sheet structure calculated for each trace are listed in Table I. The β-(29–42) peptide was not included in this study, because its c.d. spectra were insensitive to changes within the pH 1 to 10 range.

For β-(1–28), the maximum amount of helix (70 to 89%) in 60% TFE was observed at pH 1·2. The α-helix content decreases as the pH is increased from 1·2 to 4·7. The smallest amount of α-helix (28 to 32%) is reached at pH 5·4 (Table I). Concurrently, as the α-helical content drops, the β-sheet content rises, to a maximum of 60% at pH 5·4. A similar trend is seen as the pH is varied from 10·2 to 5·4. The behavior of β-(1–39) is analogous to that of β-(1–28), where a minimum of α-helix and maximum of β-sheet content is attained at approximately pH 5·5.

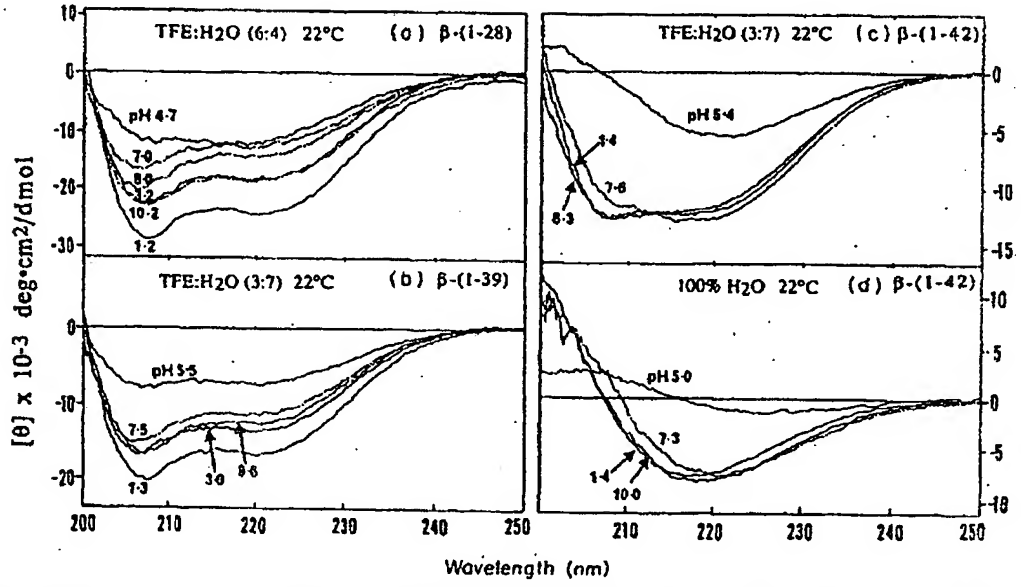

Figure 5. Effects of pH on the c.d. spectra of the β-(1–28), β-(1–39), β-(1–42) peptides. The conditions are as indicated and the amounts of secondary structures calculated for each spectra are summarized in Table I under pH study. The β-(29–42) peptide was not included in this study since its c.d. spectra are insensitive to pH. In (c), spectra obtained at pH 3·0 and 9·6 were identical to those shown for pH 1·4 and 8·3, respectively. In (d), spectra obtained at pH 3·0 and 12·0 were identical to spectra at pH 1·4 and 10·0, respectively.

Comparison of the c.d. spectra of β-(1–39) and β-(1–42) (Fig. 5(b) and (c)), demonstrates that β-(1–42) contains significantly more β-sheet content at all pH values. For example, at pH 5·4 there is 80% β-sheet content for β-(1–42) and only 40% β-sheet for β-(1–39) (Table 1). At pH 7·6, β-(1–42) contains 50% β-sheet, 23 to 38% α-helical, and 25% random coil structures, whereas β-(1–39) is 15% β-sheet, 38 to 41% α-helix, and 47% random coil.

(d) *Kinetics of β-sheet production and precipitation*

The percentages of secondary structures can alter with time, and all peptides eventually adopt complete β-sheet structure in mid-range pH values (4 to 7). The rate of β-sheet production is fastest for β-(1–42), and other factors such as peptide concentration are also important; i.e. as shown below the β-sheet conformation is oligomeric, so that solutions that contain higher peptide concentrations, will more rapidly aggregate as β-sheet.

c.d. spectra for the β-(1–42) peptide in water at pH 1·4, 5·0, 7·3 and 10·0 are shown in Figure 5(d). These spectra demonstrate that in water the β-(1–42) peptide exists almost exclusively in a β-sheet conformation. There is a progressive shift in the β-sheet minimum to higher wavelengths as the pH is raised or lowered toward mid-range values (4 to 7). The highest wavelength is seen at 226 nm at pH 5·0, and the intensity of this band is also reduced. This wavelength shift and subsequent reduction in intensity occurs because β-(1–42) is forming large aggregates that ultimately precipitate from solution. In separate experiments, c.d. spectra were recorded in 100% water at pH 5·5 as a function of time, and progressive decreases in the intensity of the c.d. band at 217 to 222 nm, together with a shift to longer wavelengths, were observed. For a 12 μM sample of β-(1–42) there was a constant rate of aggregation, so that after two hours at 22°C a spectrum equivalent to the baseline was obtained. Centrifugation of the solution showed that the peptide had precipitated as a white solid, which could only be dissolved in strong acid, such as trifluoroacetic acid or formic acid. The rate of aggregation, monitored by the c.d. changes and precipitate formation, decreased as the pH was altered in either direction from pH 5·0. In highly basic (pH 8 to 12) or acidic (pH 1 to 3) medium, β-(1–42) was essentially β-sheet, but the c.d. spectra were reproducible and no precipitate formed. Solutions kept near physiological pH (for example, at pH 7·3) precipitated slower than if kept at acidic pH. The same trends were found for solutions of β-(1–42) in 25% TFE-water (Fig. 5(c)).

(e) *Effects of temperature*

The enthalpic contribution to the α-helical structure was estimated by recording c.d. spectra at different temperatures. Shown in Figure 6 are thermal unfolding curves for the α-helical structures

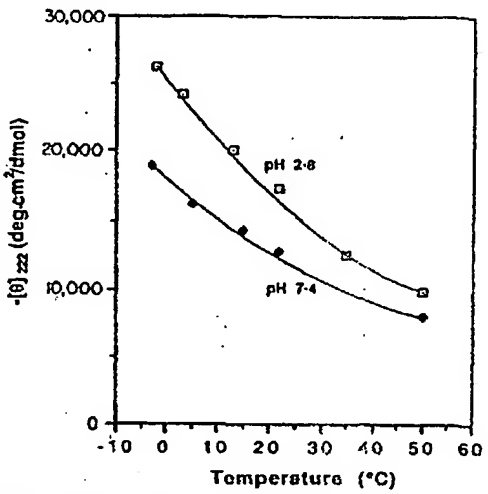

Figure 6. Temperature dependence of helix formation for β-(1–28) in 60% TFE, 22°C, at pH 2·8 (upper curve) and at pH 7·4 (lower curve). Peptide concentration was 4·3 μM (see Table 1 for data).

of β-(1–28) at pH 2·8 and 7·4 in TFE-water solutions. The data are listed in Table 1. More α-helix is seen at pH 2·8 than at pH 7·4, with maximum α-helix observed at −3°C. The lack of a low temperature plateau implies that maximum α-helical content has not yet been reached. With increasing temperature at pH 2·8, the α-helical content falls rapidly, and this drop in α-helical structure is accompanied by an increase in random coil structure (Table 1). By contrast, with increasing temperature at pH 7·4, a smaller drop in α-helical content is observed, accompanied by increases in both random coil and β-sheet structures. Approximately 30% α-helix remains at 50°C, and both curves start to decrease in slope at higher temperatures, implying a limit to the breakdown of α-helical structure. This suggests that β-(1–28) may contain two α-helical regions, one of which is more stable to temperature increases than the other.

(f) *Concentration dependence of α-helix and β-sheet formation and time-dependent c.d. studies*

To explore the possibility of intermolecular structure formation, studies of α-helix and β-sheet formation as a function of peptide concentration were performed. A plot of the percentage α-helix of β-(1–28) at pH 2·8, 5·4 and 7·4 are shown in Figure 7(a), and the data are summarized in Table 1. These studies were carried out in 60% TFE solution, which are solvent conditions designed to optimize helix formation and minimize the co-occurrence of other secondary structures (see section (b), above). A graph showing the effect of peptide concentration on the percentage β-sheet structure for β-(1–28) at pH 5·4 is depicted in Figure 7(b). Data for the β-(29–42) peptide are also shown on the same graph

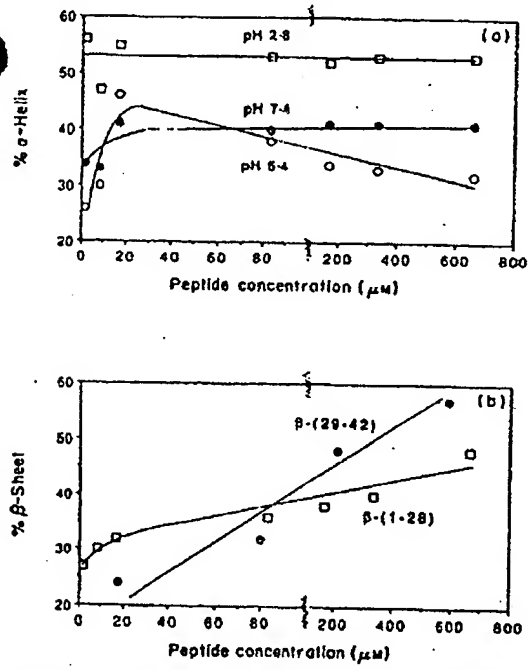

Figure 7. Variations of α-helical (a) and β-sheet (b) content as a function of peptide concentration. The data for helical content (a) were obtained with the β-(1–28) peptide in 60% TFE, 22°C, and at the pH values as indicated. The data for β-sheet content (b) were obtained at 22°C with the β-(1–28) peptide in 60% TFE at pH 5·4 (maximum for β-sheet formation), and the β-(29–42) peptide in 60% HFIP at pH 7·3. The percentages of secondary structures and peptide concentrations are listed under Peptide concentration study in Table 1.

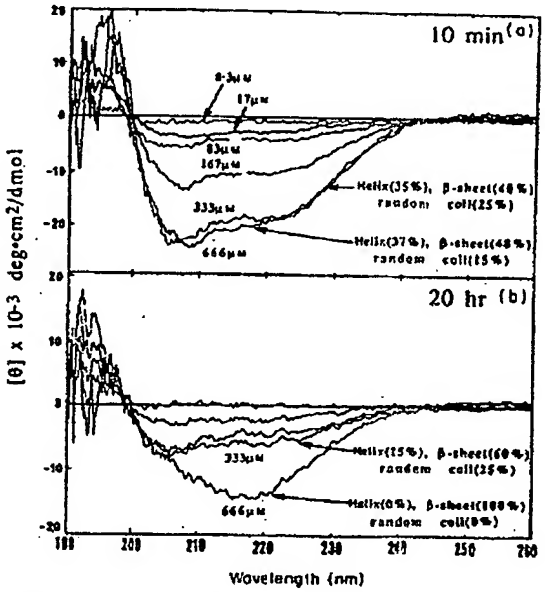

Figure 8. c.d. spectra recorded with different peptide concentrations of β-(1–28) in 60% TFE at pH 5·4. The spectra shown in the upper panel (a) were recorded 10 min after peptide dissolution, while the lower panel (b) contains spectra for the identical samples recorded 20 h after peptide dissolution. The secondary structures deduced from the spectra in (a) were also used in the graphs of Fig. 7. To reduce overlap, the bottom panel (b) does not include spectra for the 8·3 μM-β-(1–28) sample.

(Fig. 7(b)). This experiment was repeated three times and the results were reproducible ± 10%.

The β-(1–28) peptide at pH 2·8 and 7·4 has 46 to 58% and 41 to 47% α-helix, respectively, with the remainder being random coil. The conformation was independent of peptide concentration throughout the 1·7 to 666 μM range. These solutions were stable over time, and no changes in the relative amounts of α-helix and random coil were observed over a two month period. Within the pH 4·3 to 6·7 range, however, mixtures of β-sheet, α-helix and random coil co-exist in solution (Table 1). Moreover, for peptide solutions kept at pH 4·3 to 6·7, the relative proportions of α-helix, β-sheet, and random coil are both time and concentration-dependent.

Shown in Figure 8(a) (upper) are c.d. spectra of β-(1–28) recorded at pH 5·4 and with peptide concentrations of 1·7, 8·3, 17·0, 83·0, 167·0, 333·0 and 666·0 μM. The relative amounts of secondary structures for each solution are listed in Table 1. The 333 μM and 666 μM solutions contain similar amounts of α-helix, but slightly different amounts of β-sheet and random coil. All of these spectra were recorded ten minutes after peptide dissolution. c.d. spectra were again obtained after allowing the solutions to stand at room temperature for 20 hours. The spectra are shown in Figure 8(b) (lower) and the amounts of secondary structures calculated for the 333 and 666 μM solutions are also shown. Only the two most concentrated solutions show significant conformational changes over time, both increasing in β-sheet content. After 20 hours the 666 μM solution contains peptide that is fully β-sheet. These results show that the rate of β-sheet formation and subsequent aggregation is concentration-dependent.

(g) *Molecular weight determination by size exclusion chromatography*

As an adjunct to the above c.d. concentration studies, the apparent molecular weights of β-(1–28), β-(1–39) and β-(1–42) were measured by chromatography on a Sephadex G50F column at pH 3·5 and 7·4. The column was calibrated with pepsin (34,700), lysozyme (14,300), adrenocorticotropic hormone (4567) and melanocyte-stimulating hormone (1665). A representative elution profile for β-(1–28) at pH 7·4, and the calibration curve for the column at pH 7·4 are shown in Figure 9. From interpolation of calibration curves at pH 7·4 and 3·5, the apparent molecular weights of the peptides were obtained, then divided by their nominal weights to give the

Table 2
Size exclusion chromatography data for amyloid β-peptides in aqueous solution

Peptide	pH	Average monomeric MW (daltons)†	Experimental MW (daltons ±10%)‡	Degree of aggregation§
β-(1–28)	3·5	3262	3800	1·2
	7·4		3680, 13120	1·1, 4·0
β-(1–39)	3·5	4235	4400	1·0
	7·4		4400, 9120, 13120, 18880	1·0, 2·2, 3·1, 4·4
β-(1–42)	3·5	4515	4800	1·1
	7·4		4400, 9120, 13120, 18880	0·97, 2·0, 2·9, 4·2

Due to its poor solubility in the aqueous buffer, the β-(29–42) peptide was not included in this study.
† Obtained from MS measurements (see Materials and Methods).
‡ The molecular weights (MW) are accurate ±10%.
§ Degree of aggregation = experimental molecular weight/theoretical monomeric molecular weight.

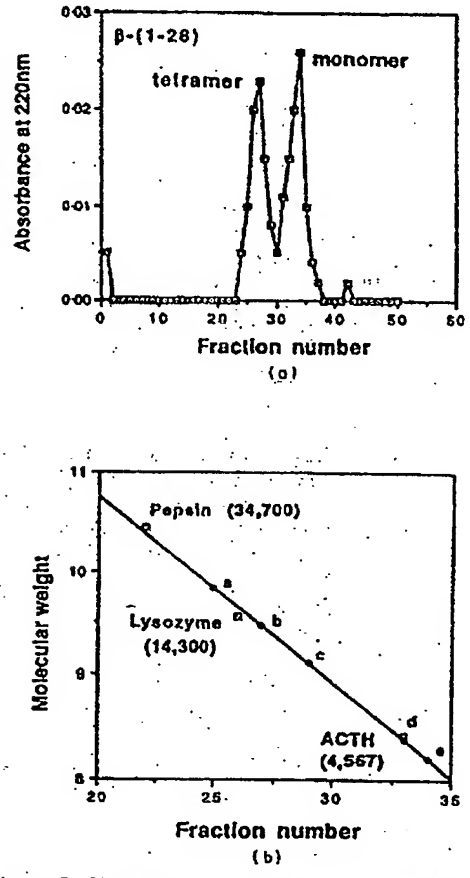

Figure 9. Size-exclusion chromatography data of the amyloid β-peptides (except β-(29–42)) in aqueous solution at pH 7·4 (see Table 2 for data). The upper plot (a) is an elution profile for the β-(1–28) peptide. The lower graph (b) is a calibration curve showing peaks for the standards (pepsin, lysozyme, adrenocorticotropic hormone (ACTH)); also, peak a corresponds to tetrameric β-(1–39) and β-(1–42); peak b corresponds to tetrameric β-(1–28) and trimeric β-(1–39) and β-(1–42); peak c corresponds to dimeric β-(1–39) and β-(1–42); peak d corresponds to monomeric β-(1–39) and β-(1–42); peak e corresponds to monomeric β-(1–28).

aggregation numbers reported in Table 2. The two peaks for β-(1–28) at pH 7·4 (Fig. 9(a), upper) had molecular weights of 3674 and 13,124, consistent with a monomer and a tetramer, respectively. The β-(1–39) and β-(1–42) peptides had four peaks in their elution profiles at pH 7·4, which corresponded to more complex mixtures of monomers, dimers, trimers and tetramers (Table 2). In contrast, the data obtained at pH 3·5 established that all three peptides are monomeric.

4. Discussion

(a) *Previous research on β-peptide and its fragments*

Previously reported secondary structure predictions for β-peptide (Kirschner *et al.*, 1987; Gorevic *et al.*, 1987), together with our own predictions, show no dominant conformation for β-peptide. Most importantly, our results show that the solution environment clearly overrides predicted conformational tendencies, so prediction alone is not a valid method for secondary determinations for β-peptide and its analogs.

In the solid state, the β-(1–28), β-(12–28), β-(14–28), β-(6–25), β-(1–38) and β-(1–40) peptides (Kirschner *et al.*, 1987; Gorevic *et al.*, 1987; Fraser *et al.*, 1991*a*) all formed amyloid-like fibrils *in vitro*. Other shorter peptides, β-(16–28) and β-(18–28), form broad ribbon-like structures, unlike the natural amyloid filaments (Gorevic *et al.*, 1987). Based upon these results, it was proposed that the N-terminal β-(1–28) segment conferred amyloidogenic potential to β-peptide. Halverson *et al.* (1990) have shown that the β-(34–42) segment adopts antiparallel β-sheet structures, indicating that the C-terminal region likewise confers some amyloidogenic potential. More recently, Fraser *et al.* (1991*b*) and Burdick *et al.* (1992) have demonstrated that fibril assembly and disassembly is pH-dependent, with β-sheet/fibril formation occurring only between pH 3 to 8. These latter results are analogous to the work shown here, and to other previous work which we had reported earlier (Barrow & Zagorski, 1991).

To our knowledge, only two reports have attempted to describe the structure of the amyloid

β-peptides in solution. In the first published report, using c.d. the β-(1–28) peptide was reported to have a maximum α-helical content of 23% in TFE-water mixtures (Hollosi *et al.*, 1989). These results disagree with our work in that we observe greater amounts of α-helix. In addition, there was no mention of changes in structure with variations in pH or temperature, and no spectra were taken in water alone.

In the second published report, Hilbich *et al.* (1991) conducted a more thorough investigation of the solution conformations of the amyloid β-peptides. Using solubility determinations, electron microscopy, infrared (IR) spectroscopy, and c.d., they demonstrated that residues 10 to 43 form a prototype for the natural β-peptide; the β-(10–43) peptide in water forms a dimer that is 80% β-sheet, 10% turn I, and 10% random coil conformation. This essentially agrees with our results for β-(1–42). However, using the results from chromatographic separation, Hilbich *et al.* (1991) concluded that "the solubilities and structures of the peptides were dependent on salt concentration, but seemed not to be affected by pH differences in the range tested", which were pH 4·5, 6·1, or 9·3. In the present study, using c.d., we have shown that the secondary structures vary with pH in a time-dependent fashion (Fig. 8), where mixtures of α-helix, β-sheet, and random coil co-exist in solution. We also found, in contrast to Hilbich *et al.* (1991), that solutions with higher peptide concentrations favor production of the β-sheet conformation. Their failure to take time-dependent factors into account may explain why alterations of secondary structure with pH were not detected in their study.

(b) *Stability of α-helix and β-sheet structures*

It is clear from the solvent composition studies that the fluorinated alcohols (TFE and HFIP) favor production of the α-helical structure at the expense of the random coil and β-sheet structures. There are differences with regard to TFE and HFIP, in that less HFIP is generally required to stabilize the α-helical structure. However, the maximum α-helical content obtained with HFIP or TFE are nearly identical, showing that HFIP does not cause additional α-helix formation, consistent with the current understanding that these solvents do not induce α-helix formation. The hydrophobic β-(29–42) peptide has a progressive shift from a β-sheet structure to random coil with proportionate increases of either TFE or HFIP. Since these solvents promote intramolecular hydrogen-bonding, these results indicate that the α-helical conformation is intramolecular, whereas the β-sheet structure is intermolecular.

TFE and HFIP are well known for stabilizing α-helices that are in equilibrium with random coil structures. These solvents are weaker proton donors than water, and promote structure formation by allowing intramolecular hydrogen-bonding to occur, rather than intermolecular hydrogen-bonding with solvent. Most importantly, these solvents do not *induce* helix formation, but more correctly, *stabilize* α-helices in regions that have an intrinsic tendency to assume helical conformation, such as regions that form "nascent helices" in water (Dyson *et al.*, 1988).

Helix formation is an enthalpy-driven process with unfolding of the helix increasing with increasing temperature. In contrast, changes in temperature had no effect on the β-sheet conformation. Rapid breakdown of secondary structure with increasing temperature usually indicates that hydrophobic interactions are not important in stabilization (Bierzynski *et al.*, 1982). Thus, hydrophobic interactions are probably important for stabilization and formation of the β-sheet conformation, but are not important for the α-helical conformation.

Helical structure is formed more easily in β-(1–39) than in β-(1–42), indicating that β-(1–42) forms a more stable β-sheet structure. In water, there is approximately 25% less β-sheet structure for β-(1–39), and less amounts of TFE or HFIP are required to disrupt the β-sheet structure and produce α-helical structure. Moreover, the influence of TFE on the secondary structures of β-(1–39) and β-(1–28) are quite similar. This suggests that the Val40-Ile41-Ala42 segment is critical for stabilization of the β-sheet structure in solution, which is most likely the structure formed prior to the β-pleated sheet structure of amyloid deposits. It is possible that the less soluble β-(1–42) peptide (the major form in plaque core amyloid) is the product from a defective proteolysis of APP that occurs during AD, while the β-(1–39) peptide (the major form in vascular amyloid) is the product from a normal proteolysis of APP. This proposition is supported by Abraham (1989), where it was implied that only a β-peptide containing a minimum of 42 to 43 amino acids could induce a neuritic response.

(c) *Aggregation states of the α-helix and β-sheet conformations*

The rates and amounts of β-sheet formation are dependent upon peptide concentration (Fig. 7). This dependency is more pronounced for the completely hydrophobic β-(29–42) peptide, than for the less hydrophobic β-(1–28) peptide. These results suggest that the β-sheet conformation in solution is an inter- and not an intramolecular structure. This also agrees with the results of the solvent studies discussed above, where TFE and HFIP, which promote intramolecular hydrogen bonding, disfavor production of the β-sheet structure. It is likely that the intermolecular β-sheet structure in solution is a precursor to the intermolecular cross-β-pleated sheet structure in amyloid deposits (Kirschner *et al.*, 1986).

Helix formation is monomeric at pH 2·8 and 7·4 over the peptide concentration range of 1·7 to 666 μM for the β-(1–28) peptide (Fig. 7). The data obtained at pH 5·4, however, are unusual in that the amount of α-helical structure rises from 26 to 46%

for peptide concentrations of 1·7 to 17 μM, respectively, then drops to 32% at 666 μM (Fig. 7). This latter drop in α-helical content may be due to the co-occurrence of β-sheet structure, which for the β-(1–28) peptide is expected at pH 5·4, but not at pH 2·8 or 7·4 (Fig. 5). According to the size-exclusion chromatography data (Table 2), at pH 3·5 only monomeric species exist in solution, which agrees with the c.d. data, but at pH 7·3 a mixture of monomers, dimers, trimers and tetramers may co-exist in solution (Table 2). These results agree qualitatively with work by Masters *et al.* (1985), where gel permeation chromatography demonstrated that monomeric forms exist at low pH, but dimeric and tetrameric forms are present at neutral and high pH. Together, these results indicate that the peptides at high pH (7 to 10), even when containing considerable α-helix, are a mixture of monomers, dimers, trimers and tetramers, while at low pH (1 to 4) only monomeric peptide is present. From these results we cannot say whether the aggregation observed is due to intermolecular interactions between helices or interactions between small β-sheet regions within the peptides.

(d) *Reversibility of α-helix to β-sheet transition*

Helix formation is favored at pH 1 to 4 and 7 to 10, whereas β-sheet formation is favored at pH 4 to 7 (Fig. 5). For the β-(1–28), β-(1–39), and β-(1–42) peptides, at pH 4 to 7 in TFE/water solution, a mixture of α-helix, β-sheet and random coil structures co-exist in equilibrium. Over time this equilibrium moves toward more β-sheet structure, in a concentration-dependent manner (Fig. 8). Interestingly, the maximum rates of aggregation are observed at approximately pH 5·5, which is close to the predicted (Sillero & Ribeiro, 1989) isoelectric point of 6·1 for β-peptide. This indicates that a net charge of zero favors β-sheet formation.

If the peptide concentrations are relatively low (1 to 100 μM), by adjusting the pH one can cause the β-sheet content to decrease and observe a corresponding increase in the α-helical content. However, when dealing with more concentrated peptide solutions (1 to 5 mM), the transition from α-helix to β-sheet is not so readily reversible. For example, when the pH was increased from 3·5 → 4·5 or decreased from 7·1 → 6·6 for a 3·5 mM solution of β-(1–28) in TFE/water solution, the sample immediately turned into a gel that could only be dissolved in concentrated acid. The gel is presumably an amyloid-like aggregated β-sheet structure. Kirschner *et al.* (1987) performed X-ray diffraction and electron microscopy of similar gels, and found cross-β-pleated sheet structures similar to *in vivo* amyloid.

Rates of aggregation to a precipitated β-sheet structure are fastest for β-(29–42) and slowest for β-(1–28), for the four peptides studied; i.e. β-(29–42) > β-(1–42) > β-(1–39) > β-(1–28). Other factors such as peptide concentration, pH, temperature, solvent, and ionic strength are also important. More detailed time-dependent c.d. studies, which take all of these variables into account, are clearly needed to ascertain better the rates of aggregation and the degree of reversibility (β-sheet → α-helix).

(e) *Role of the hydrophobic C terminus in directing the folding to the β-pleated sheet structure in amyloid deposits*

It was proposed that β-peptide contains the major structural requirements for aggregation into amyloid filaments *in vitro* (Glenner, 1980). We have shown that the two peptide regions, β-(29–42) and β-(1–28), are quite different in their solution behavior, and that β-(29–42) has a high propensity to form β-sheet structure in aqueous solutions. This suggests that the 29 to 42 amino acid segment directs the folding of β-peptide prior to plaque formation, and predisposes the complete peptide to aggregate as the β-pleated sheet structure found in amyloid deposits. Furthermore, this segment is completely hydrophobic, and globular proteins are known to fold and form β-pleated sheets by mechanisms that involve hydrophobic interactions between adjoining segments of secondary structures (Sternberg & Thornton, 1977; Kim & Baldwin, 1990). We propose that the initial interactions between β-peptide molecules involve the C-terminal ends of two strands. After this initial interaction, if solution conditions are favorable, the remaining residues form β-structure, eventually generating the anti-parallel alignment seen in plaques.

(f) *Circulation of β-peptide in vivo; existence of the α-helical structure*

Recently, amyloid deposits containing β-peptide were detected in tissues other than the brain (Joachim *et al.*, 1989). The rationale behind these observations was that a circulating form of APP or β-peptide is responsible. APP has been found in human platelets (Bush *et al.*, 1990; Gardella *et al.*, 1990) and mononuclear blood leucocytes (Mönning *et al.*, 1990). In addition, large soluble fragments of APP are known (Dyrks *et al.*, 1988; Selkoe *et al.*, 1988; Palmert *et al.*, 1989), although most of these fragments do not contain the full β-peptide segment, and therefore cannot serve as precursors of the β-peptides found in plaques (Ishiura, 1991).

Our work establishes that β-peptide alone may be soluble enough for transportation in blood. At low concentrations β-peptide could be transported in a β-sheet conformation. This is the conformation expected in blood plasma, since at physiological pH in water the natural peptides, β-(1–39) and β-(1–42), adopt primarily β-sheet conformations (Table 1). Alternatively, the peptides could be transported in blood in an α-helical conformation. This latter possibility may occur if β-peptide were associated with lipid material, where β-peptide would be expected to be α-helical, as in the membrane mimicking TFE/water mixtures (Braun *et al.*, 1983). Residues 8 to 17 of β-peptide can associate and bind to lipid

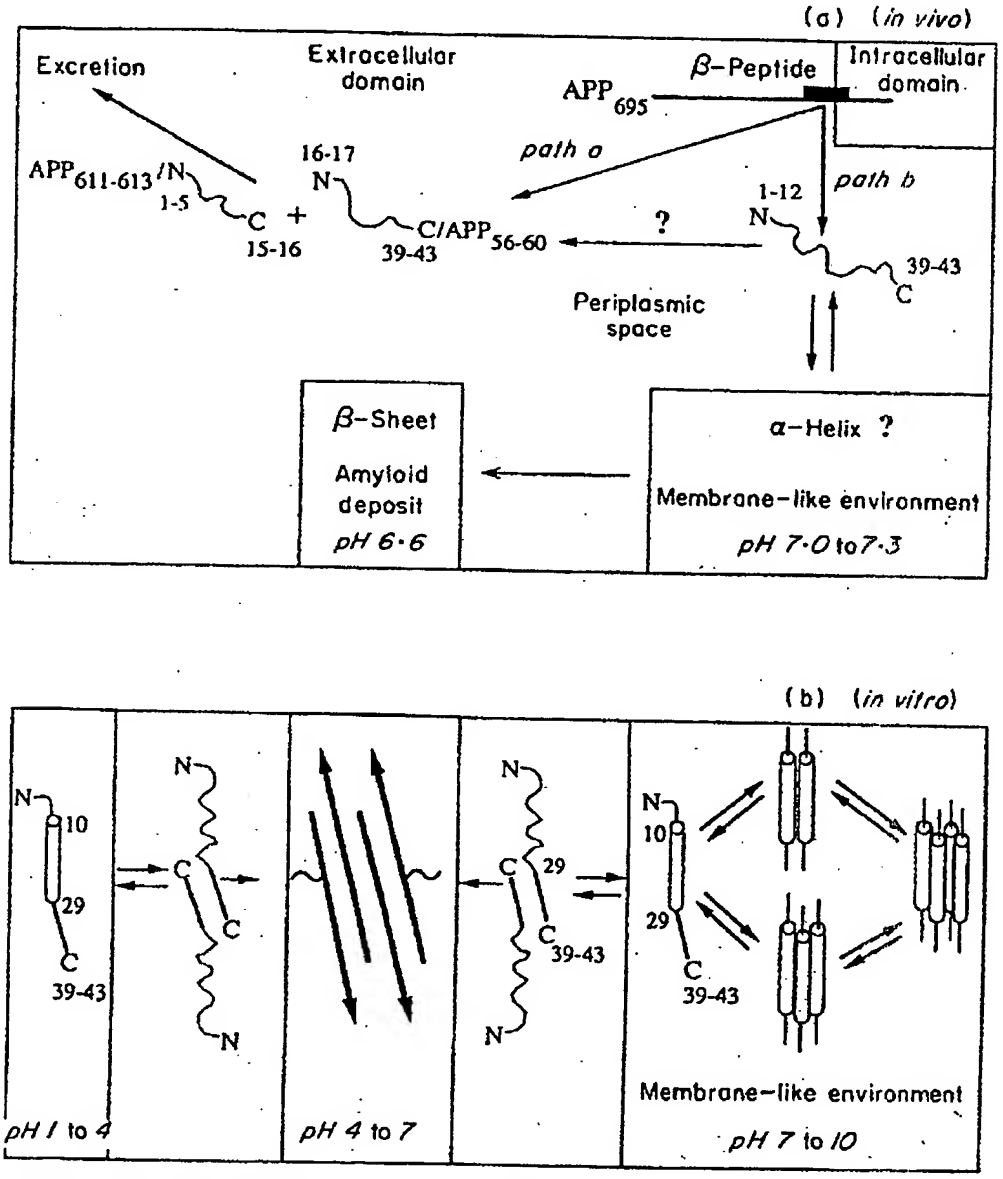

Figure 10. Scheme for production of amyloid in AD that suggests β-peptide can remain solubilized in a membrane-like environment, and that a reduction in pH 7·3 → 6·6 accelerates amyloid plaque formation. The pH 6·6 value, as drawn in the amyloid deposit (upper, (a)), was recently demonstrated to exist in AD brain (Yates *et al.*, 1990). The upper scheme (a) pertains to a possible *in vivo* situation, while the lower scheme (b) pertains to an *in vitro* situation according to the results shown here. In the upper scheme (a), *path a* corresponds to proteolysis of APP within residues 15 to 17 of β-peptide to produce soluble fragments that after further proteolysis can be excreted (Sisodia *et al.*, 1990; Esch *et al.*, 1990), and *path b* corresponds to a proteolysis of APP that releases β-peptide with heterogeneous termini. Since the *in vivo* proteolysis of β-peptide, as well as its existence *in vivo* in an α-helical conformation, have yet to be demonstrated, question marks (?) are drawn. We suggest that once β-peptide forms, it may either undergo further cleavage with subsequent excretion, or be transported in blood within a membrane-like environment (in an α-helical conformation). If an abnormal solution condition develops, such as a drop in pH, then β-peptide may spontaneously aggregate and precipitate as an amyloid deposit (in a β-sheet conformation). In the lower scheme (b), α-helices are drawn with cylinders, and the antiparallel β-sheet conformations are drawn with continuous lines running in opposite directions. The favored conformations of β-peptide at 3 ranges of pH (1 to 4, 4 to 7, and 7 to 10) are shown. Evidence for the helix-helix interactions shown at pH 7 to 10, as well as the location of the helix within residues 10 to 28 (lower (b)), are based upon n.m.r. studies (Barrow & Zagorski, 1991). This scheme also implies that the hydrophobic residues 29 to 42 make the initial contact prior to formation of the β-pleated sheet structure of amyloid deposits; for simplicity, these initial interactions are depicted as antiparallel.

receptors (Allsop *et al.*, 1988); also, the 29 to 42 segment should interact favorably with lipids or membranes, as this segment is hydrophobic and naturally membrane-bound in APP.

We propose that once released from APP, β-peptide could become localized within a membrane-like environment, and subsequently transported to different regions of the body in blood (Fig. 10). In this way blood would provide a suitable environment for β-peptide to exist in a soluble, monomeric α-helical conformation. This proposition means that we do not need to envisage the existence of a common circulating precursor to β-peptide.

(g) *Mechanism of pH-induced amyloidogenesis*

The pathogenesis and the mechanism of amyloid formation in AD is unknown (for reviews, see Wisniewski & Iqbal, 1980; Castano & Frangione, 1988). Current theories assume that an abnormal cleavage of APP occurs so that β-peptide is released, and then spontaneously aggregates into amyloid deposits. Support for these theories comes from several recent findings: (1) two forms of APP (APP751 and APP770) contain Kunitz-type protease inhibitor domains (Kitaguchi *et al.*, 1988); (2) proteolytic cleavage to residue 16 of β-peptide within APP was demonstrated (Sisodia *et al.*, 1990; Esch *et al.*, 1990); (3) several protease inhibitors, such as α_1-antichymotrypsin (Abraham *et al.*, 1988) and cathepsin B and D (Cataldo & Nixon, 1990), are present in amyloid deposits of AD. However, the roles of these protease inhibitors in the production of amyloid have yet to be determined. Also, the suggestion that cleavage within the amino acid region of β-peptide is the normal processing of APP is still speculative.

Outlined in Figure 10(a) are two cleavages of APP (for simplification, shown only for APP695). As mentioned above, one known cleavage (Fig. 10(a), *path a*) involves proteolysis of APP between Gln15 and Leu17 of β-peptide, where the intervening Lys16 is removed by an exopeptidase (Sisodia *et al.*, 1990; Esch *et al.*, 1990). The second cleavage of APP (Fig. 10(a), *path b*) releases β-peptide. The cleavage sites for the latter path are quite variable, with both the N- and C-terminal ends being heterogeneous (Kang *et al.*, 1987; Prelli *et al.*, 1988). Once released, β-peptide could be secreted into blood, internalized by cells, or itself undergo further proteolysis. If internalized by cells or present in blood serum, we propose that β-peptide may become localized in a membrane-like environment, where it can adopt a stable α-helical conformation (Fig. 10(a)), analogous to its conformation in TFE/water (Fig. 10(b)). In an α-helical conformation, β-peptide would remain in solution, and could be transported in blood. It should be kept in mind that neither soluble β-peptide forms, nor a common circulating precursor, have yet been detected in blood.

In either an aqueous or a membrane-like environment β-peptide favors a β-sheet structure at pH 4 to 7 (Fig. 5). We estimate (Sillero & Ribeiro, 1989) that the isoelectric point of β-peptide is approximately 6·1, similar to pH 5·5 where a maximum in aggregation of β-(1–42) is observed. Perhaps the approach of the brain microenvironment pH towards the isoelectric point of β-peptide is responsible for the aggregating interactions.

Yates *et al.* (1990) have shown that brains from patients who die after Alzheimer disease are more acidic (pH 6·6) than brains from patients who die suddenly with no brain disease (pH 7·1). This result is especially significant, because our work has shown that the rate of aggregation of β-peptide would be greater at pH 6·6 than at pH 7·1. Thus, a drop in pH (7·1 → 6·6) should speed up amyloid plaque formation *in vivo* (Fig. 10(a)). It is also known that β-peptide can exist in distinct states of aggregation within different lesions (Spillantini *et al.*, 1990). This means that β-peptide probably aggregates to form plaques in stages, initially forming preamyloid deposits (Yamaguchi *et al.*, 1988; Tagliavini *et al.*, 1988; Mann & Esiri, 1988). Under normal conditions, these preamyloid deposits may be soluble enough to be excreted from the body, either *via* proteolysis or another mechanism. However, changes in environmental factors, such as a lowering of pH, may induce aggregation leading to high concentrations of insoluble amyloid plaques.

Many events *in vivo* could be responsible for the localized fluctuations in pH that cause β-peptide to precipitate as amyloid. For example, decreases in the supply of oxygen (ischemia) to cerebral tissue are usually accompanied by reductions in pH (Gilboe *et al.*, 1986); i.e. drops of pH 7·1 → 6·0 have been described (Munekata & Hossmann, 1987). When ischemia is accompanied by elevated blood glucose levels (hyperglycemia), cerebral pH can fall even lower to pH 5·2 to 5·4 for a period of 20 minutes (Kraig *et al.*, 1987). Moreover, both ischemia and hyperglycemia, as well as shock, hypotension, hypoxia and renal disorders which all also lower blood pH (Johnston & Alberti, 1983), are typically found in elderly patients where the incidence of AD is greatest. Other possibilities include epileptic seizures (Siesjö, 1985), changes in localized neurotransmitter concentrations, contact with neutrophils and monocytes where the pH can drop to as low as 4·5 to 5·0 (Jacques & Bainton, 1978), or degenerating neurons which can alter the pH by releasing cathepsin-laden vesicles (Cataldo & Nixon, 1990).

For the transition α-helix → random coil → β-sheet as the pH is lowered from 7·0, it is likely that one or more histidine residues are being protonated. One possibility is that within the α-helix, a histidine residue (expected pK_a in a protein is 6·5 to 7·0) could be involved in an electrostatic interaction with a carboxylate group of an adjacent monomer. If this is the case, then increases in ionic strength should promote disruption of the dimers, trimers and tetramers of the α-helix into monomers. In this regard, Hilbich *et al.* (1991) observed only monomers with high salt concentrations. We are currently re-examining the effects of

ionic strength of the secondary structures of β-peptide inside the pH 7 to 10 range.

Our work shows that β-peptide can form aggregated β-sheet structures *in vitro*. Thus, materials such as aluminum, heparan, lipids or other proteins, which are normally found colocalized in the amyloid deposits (Candy *et al*, 1986; Behrouz *et al*., 1989), may not be critical for the deposition of β-peptide *in vivo*. Instead, they probably facilitate the process by serving as additional nucleating centers as β-peptide begins to precipitate into an amyloid deposit. We suggest that β-peptide deposition is a late-stage neuronal event, which is induced by environmental factors. If a drop in pH is necessary for amyloid deposition, then correcting it may provide a therapeutic means to prevent amyloid accumulation and perhaps slow the progress of Alzheimer's disease.

5. Conclusions

This study reports on c.d. investigations of the solution conformations of synthetic β-peptides. The results from our work demonstrate that β-peptide is *not* an intrinsically insoluble protein, and that it adopts different conformations in solution depending upon the external solution conditions. We have shown that environmental pH is an important factor in the rate of β-peptide aggregation, with the most rapid aggregation occurring close to the isoelectric point of β-peptide. Our results also suggest that β-peptide alone is soluble enough to be transported in blood. The present study underscores the need for further research into the conformation, dynamics and mechanisms of amyloidosis of β-peptide in solution and, in particular, for more detailed studies on a molecular level. Such information could be applicable to the design of drugs to curtail the amyloidosis of β-peptide *in vivo*.

We thank Drs Vassil Vassilev (SUNBOR) and Koji Nakanishi (Director, SUNBOR) for many helpful discussions. We are also extremely grateful to Dr Ron Orlando (SUNBOR) for his assistance in obtaining the MS-MS data, and to Dr Takashi Takakuwa (Jasco, Inc.) for providing the c.d. reference files for poly-L-lysine.

References

Abraham, C. R. (1989). Potential roles of protease inhibitors in Alzheimer's disease. *Neurobiol. Aging*, **10**, 463–465.

Abraham, C. R., Selkoe, D. J. & Potter, H. (1988). Immunochemical identification of the serine protease inhibitor α_1-antichymotrypsin in the brain amyloid deposits of Alzheimer's disease. *Cell*, **52**, 487–501.

Allsop, D., Wong, C. W., Ikeda, S.-I., Landon, M., Kidd, M. & Glenner, G. G. (1988). Immunohistochemical evidence for the derivation of a peptide ligand from the amyloid β-protein precursor of Alzheimer's disease. *Proc. Nat. Acad. Sci., U.S.A.* **85**, 2790–2794.

Barrow, C. J. & Zagorski, M. G. (1991). Solution structures of β peptide and its constituent fragments: relation to amyloid deposition. *Science*, **253**, 179–182.

Behrouz, N., Defossez, A., Delacourte, A., Hublau, P. & Mazzuca, M. (1989). Methods in laboratory investigation, Alzheimer's disease: glycolytic pretreatment dramatically enhances immunolabeling of senile plaques and cerebrovascular amyloid substance. *Lab. Invest. U.S.A.* **61**, 576–583.

Bierzynski, A., Kim, P. S. & Baldwin, R. L. (1982). A salt bridge stabilizes the helix formed by isolated C-peptide of RNase A. *Proc. Nat. Acad. Sci., U.S.A.* **79**, 2470–2474.

Brahms, S. & Brahms, J. (1980). Determination of protein secondary structure in solution by vacuum ultraviolet circular dichroism. *J. Mol. Biol.* **138**, 149–178.

Braun, W., Wider, G., Lee, K. H. & Wüthrich, K. (1983). Conformation of glucagon in a lipid-water interphase by proton nuclear magnetic resonance. *J. Mol. Biol.* **191**, 553–561.

Burdick, D., Soreghan, B., Kwon, M., Kosmoski, J., Knauer, M., Henschen, A., Yates, J., Cotman, C. & Glabe, C. (1992). Assembly and aggregational properties of synthetic Alzheimer's A4/β amyloid peptide analogs. *J. Biol. Chem.* **267**, 546–554.

Bush, A. I., Martins, R. N., Rumble, B., Moir, R., Fuller, S., Milward, E., Currie, J., Ames, D., Weidemann, A., Fischer, P., Multhaup, G., Beyreuther, K. & Masters, C. L. (1990). The amyloid precursor protein of Alzheimer's disease is released by human platelets. *J. Biol. Chem.* **265**, 15977–15983.

Candy, J. M., Klinowski, J., Perry, R. H., Perry, E. K., Fairbairn, A., Oakley, A. E., Carpenter, T. A., Atack, J. R., Blessed, G. & Edwardson, J. A. (1986). Aluminosilicates contribute to senile plaque formation in Alzheimer's disease. *Lancet*, **i**, 354–356.

Castano, E. M. & Frangione, B. (1988). Human amyloidosis, Alzheimer's disease and related disorders. *Lab. Invest.* **58**, 122–132.

Cataldo, A. M. & Nixon, R. A. (1990). Enzymatically active lysosomal proteases are associated with amyloid deposits in Alzheimer brain. *Proc. Nat. Acad. Sci., U.S.A.* **87**, 3861–3865.

Chang, C. T., Wu, C.-S. C. & Yang, J. T. (1978). Circular dichroic analysis of protein conformation: inclusion of the β-turns. *Anal. Biochem.* **91**, 13–31.

Coria, F., Castano, E. M. & Frangione, B. (1988). Brain amyloid in normal aging and cerebral amyloid angiopathy is antigenetically related to Alzheimer's disease β-protein. *Amer. J. Path.* **129**, 422–428.

Dyrks, T., Weidemann, A., Multhaup, G., Salbaum, J. M., Lemaire, H.-G., Kang, J., Müller-Hill, B., Masters, C. L. & Beyreuther, K. (1988). Identification, transmembrane orientation and biogenesis of the amyloid A4 precursor of Alzheimer's disease. *EMBO J.* **7**, 949–957.

Dyson, J., Rance, M., Houghton, R. A., Lerner, R. A. & Wright, P. E. (1988). Folding of immunogenic peptide fragments of proteins in water solution. II. The nascent helix. *J. Mol. Biol.* **201**, 201–217.

Esch, F., Keim, P. S., Beattie, E. C., Blacher, R. W., Culwell, A. R., Oltersdorf, T., McClure, D. & Ward, P. J. (1990). Cleavage of amyloid β-peptide during constitutive processing of its precursor. *Science*, **248**, 1122–1124.

Fraser, P. E., Duffy, L. K., O'Malley, M. B., Nguyen, J. T., Inouye, H. & Kirschner, D. A. (1991*a*). Morphology and antibody recognition of synthetic β-amyloid peptides. *J. Neurosci. Res.* **28**, 474–485.

Fraser, P. E., Nguyen, J. T., Surewicz, W. K. & Kirschner, D. A. (1991*b*). pH-dependent structural transitions of Alzheimer amyloid peptides. *Biophys. J.* **60**, 1190–1201.

Gardella, J. E., Ghiso, J., Gorgone, G. A., Marratta, D.,

Kaplan, A. P., Frangione, B. & Gorevic, P. D. (1990). Intact Alzheimer amyloid precursor protein (APP) is present in platelet membranes and is encoded by platelet mRNA. *Biochem. Biophys. Res. Commun.* 173, 1292–1298.

Gilboe, D. D., Kintner, D. B., Emoto, S. E. & Fitzpatrick, J. H., Jr (1986). Intracellular pH and hypoxic damage in the isolated canine brain. In *Pharmacology of Cerebral Ischemia* (Krieglstein, J., ed.), pp. 119–130, Elsevier Science Publishers B. V., New York.

Glenner, G. G. (1980). Amyloid deposits and amyloidosis. *New Engl. J. Med.* 302, 1283–1292.

Glenner, G. G. (1988). Alzheimer's disease: its proteins and genes. *Cell*, 52, 307–308.

Glenner, G. G. & Wong, C. W. (1984*a*). Alzheimer's disease: initial report of the purification and characterization of a novel cerebrovascular amyloid protein. *Biochem. Biophys. Res. Commun.* 120, 885–890.

Glenner, G. G. & Wong, C. W. (1984*b*). Alzheimer's disease and Down's syndrome: sharing of a unique cerebrovascular amyloid fibril protein. *Biochem. Biophys. Res. Commun.* 122, 1131–1135.

Gorevic, P. D., Castano, E. M., Sarma, R. & Frangione, B. (1987). Ten to fourteen residue peptides of Alzheimer's disease are sufficient for amyloid fibril formation and its characteristic X-ray diffraction pattern. *Biochem. Biophys. Res. Commun.* 147, 854–863.

Greenfield, N. & Fasman, G. D. (1969). Computed circular dichroism spectra for the evaluation of protein conformation. *Biochemistry*, 8, 4108–4116.

Halverson, K., Fraser, P. E., Kirschner, D. A. & Lansbury, P. T. (1990). Molecular determinants of amyloid deposition in Alzheimer's disease. *Biochemistry*, 29, 2639–2644.

Hilbich, C., Kisters-Woike, B., Reed, J., Masters, C. L. & Beyreuther, K. (1991). Aggregation and secondary structure of synthetic amyloid βA4 peptides of Alzheimer's disease. *J. Mol. Biol.* 218, 149–163.

Hollosi, M., Otvos, L., Kajtar, J., Percell, A. & Lee, V. M.-Y. (1989). Is amyloid deposition in Alzheimer's disease preceded by an environment-induced double conformational transition? *Peptide Res.* 2, 109–113.

Ishiura, S. (1991). Proteolytic cleavage of the Alzheimer's disease amyloid A4 precursor protein. *J. Neurochem.* 56, 363–369.

Jacques, Y. V. & Bainton, D. F. (1978). Changes in pH within the phagocytic vacuoles of human neutrophils and monocytes. *Lab. Invest.* 39, 179–185.

Joachim, C. L., Mori, H. & Selkoe, D. J. (1989). Amyloid β-protein deposition in tissues other than brain in Alzheimer's disease. *Nature (London)*, 341, 226–230.

Johnson, S. A., McNeill, T., Cordell, B. & Finch, C. E. (1990). Relation of neuronal APP-751/APP-695 mRNA ratio and neuritic plaque density in Alzheimer's disease. *Science*, 248, 854–857.

Johnston, D. G. & Alberti, K. G. M. M. (1983). Acid-base balance in metabolic acidoses. In *Clinics in Endocrinology and Metabolism*, vol. 12, pp. 267–285, Saunders, New York.

Kang, J., Lemaire, H. G., Unterbeck, A., Salbaum, J. M., Masters, C. L., Grzeschik, K. H., Multhaup, G., Beyreuther, K. & Müller-Hill, B. (1987). The precursor of Alzheimer's disease amyloid A4 protein resembles a cell-surface receptor. *Nature (London)*, 325, 733–736.

Kim, P. S. & Baldwin, R. L. (1990). Intermediates in the folding reactions of small proteins. *Annu. Rev. Biochem.* 59, 631–660.

Kirschner, D. A., Abraham, C. & Selkoe, D. J. (1986). X-ray diffraction from intraneuronal paired helical filaments and extra-neuronal amyloid fibers in Alzheimer's disease indicates a cross beta conformation. *Proc. Nat. Acad. Sci., U.S.A.* 83, 503–507.

Kirschner, D. A., Inouye, H., Duffy, L. K., Sinclair, A., Lind, M. & Selkoe, D. J. (1987). Synthetic peptide homologus to b protein from Alzheimer's disease forms amyloid-like fibrils *in vitro*. *Proc. Nat. Acad. Sci., U.S.A.* 84, 6953–6957.

Kitaguchi, N., Takahashi, Y., Tokushima, Y., Shiojiri, & Ito, H. (1988). Novel precursor of Alzheimer's disease amyloid protein shows protease inhibitory activity. *Nature (London)*, 331, 530–532.

Kitaguchi, N., Takahashi, Y., Oishi, K., Shiojiri, S., Tokushima, Y., Utsunomiya, T. & Ito, H. (1990). Enzyme specificity of proteinase inhibitor region in amyloid precursor protein of Alzheimer's disease: different properties compared with protease nexin-I. *Biochim. Biophys. Acta*, 1038, 105–113.

Klunk, W. E. & Pettegrew, J. W. (1990). Alzheimer's β-amyloid protein is covalently modified when dissolved in formic acid. *J. Neurochem.* 54, 2050–2056.

Kraig, R. P., Petito, C. K., Plum, F. & Pulsinelli, W. A. (1987). Hydrogen ions kill brain at concentrations reached in ischemia. *J. Cereb. Blood Flow Metab.* 7, 379–386.

Li, L.-K. & Spector, A. (1969). The circular dichroism of β-poly-L-lysine. *J. Amer. Chem. Soc.* 91, 220–222.

Mann, D. M. A. & Esiri, M. M. (1988). The site of the earliest lesions of Alzheimer's disease. *New Engl. Med.* 318, 789–790.

Masters, C. L., Simms, G., Weinman, N. A., Multhaup, G., McDonald, B. L. & Beyreuther, K. (1985). Amyloid plaque core protein in Alzheimer's disease and Down's syndrome. *Proc. Nat. Acad. Sci., U.S.A.* 82, 4245–4249.

Mönning, U., König, G., Prior, R., Mechler, H., Schreiter-Gasser, U., Masters, C. L. & Beyreuther, K. (1990). Synthesis and secretion of Alzheimer amyloid βA4 precursor protein by stimulated human peripheral blood leucocytes. *FEBS Letters*, 277, 261–266.

Morrisett, J. D., David, J. S. K., Pownall, H. J. & Gotto, A. M. (1973). Interaction of an apolipoprotein (apoLP-alanine) with phosphatidylcholine. *Biochemistry*, 12, 1290–1299.

Müller-Hill, B. & Beyreuther, K. (1989). Molecular biology of Alzheimer's disease. *Annu. Rev. Biochem.* 58, 287–307.

Munekata, K. & Hosamann, K.-A. (1987). Effect of 5-minute ischemia on regional pH and energy state of the gerbil brain: relation to selective vulnerability of the hippocampus. *Stroke*, 18, 412–417.

Oltersdorf, T., Ward, P. J., Henriksson, T., Beattie, E. C. Neve, R., Lieberberg, I. & Fritz, L. C. (1990). The Alzheimer's amyloid precursor protein. Identification of a stable intermediate in the biosynthetic/degradative pathway. *J. Biol. Chem.* 265, 4492–4497.

Palmert, M. R., Siedlak, S. L., Berman Podlisny, M., Greenberg, B., Shelton, E. R., Chan, H. W., Usiak, M., Selkoe, D. J., Perry, G. & Younkin, S. (1989). Soluble derivatives of the β amyloid precursor of Alzheimer's disease are labeled by antisera to the β amyloid protein. *Biochem. Biophys. Res. Commun* 156, 432–437.